



## **University of Huddersfield Repository**

Clough, David A

Non-Contact Measurement and Analysis of Machine Tool Spindles

### **Original Citation**

Clough, David A (2012) Non-Contact Measurement and Analysis of Machine Tool Spindles. Masters thesis, University of Huddersfield.

This version is available at <https://eprints.hud.ac.uk/id/eprint/18101/>

The University Repository is a digital collection of the research output of the University, available on Open Access. Copyright and Moral Rights for the items on this site are retained by the individual author and/or other copyright owners. Users may access full items free of charge; copies of full text items generally can be reproduced, displayed or performed and given to third parties in any format or medium for personal research or study, educational or not-for-profit purposes without prior permission or charge, provided:

- The authors, title and full bibliographic details is credited in any copy;
- A hyperlink and/or URL is included for the original metadata page; and
- The content is not changed in any way.

For more information, including our policy and submission procedure, please contact the Repository Team at: [E.mailbox@hud.ac.uk](mailto:E.mailbox@hud.ac.uk).

<http://eprints.hud.ac.uk/>

# Non-Contact Measurement and Analysis of Machine Tool Spindles

Submitted to

School of Computing and Engineering

of

University of Huddersfield

in partial fulfilment of the requirements for

the degree of MSc by Research

David Clough

October 2012

## Abstract

---

An increasing demand on the manufacturing industry to produce tighter tolerance parts at a consistent rate means it is necessary to gain a greater understanding of machine tool capabilities, error sources and factors affecting asset availability. The machine tool spindle can be a significant contributor to both machine tool errors and failures, resulting in a requirement for spindle error measurement.

This work is an investigation into the most significant static and dynamic errors associated with a variety of common machine tool spindles and the issues around spindle metrology in hostile manufacturing environments.

Various non-contact measurement sensors are investigated and assessed for their suitability for use in a spindle analysis system. Based on the sensor selection, new measurement hardware and analysis methods were designed and developed for affordable, robust and efficient characterisation of machine tool spindle errors.

Details of practical spindle analysis are presented and reviewed, discussing potential issues and methods of minimisation of measurement error.

## Acknowledgements

---

I would like to acknowledge the assistance of the following people whose help made this research possible.

A special thank you goes to my supervisor, Simon Fletcher for his encouragement, support and direction.

Thanks to Andrew Longstaff, John Richards and Peter Willoughby for their continued support throughout.

I would also like to thank all other members of technical and academic staff at the University of Huddersfield who aided me during the course of this research.

# Table of Contents

---

Abstract .....	2
Acknowledgements .....	3
Table of Contents.....	4
Table of Figures.....	7
Table of Tables.....	10
1.0 Introduction .....	11
1.1. Spindle Error Sources .....	13
1.1.1. Geometric Spindle Errors .....	13
1.1.2. Non-Rigid Spindle Errors .....	14
1.1.3. Spindle Thermal Errors.....	14
1.2. Chapter Conclusions.....	15
2.0 Literature Review .....	16
2.1. ISO Standards .....	16
2.1.1. Determination of Thermal Affects.....	16
2.1.2. Geometric Accuracy of Axes of Rotation .....	17
2.1.3. Determination of Vibration Levels .....	19
2.1.4. ISO Standards Conclusions .....	19
2.2. Non-Contact Sensing Technology.....	20
2.2.1. Capacitance Sensors.....	20
2.2.1. Laser Triangulation Sensors .....	21
2.2.2. Eddy Current Sensors .....	22
2.2.3. Eddy Current Sensor Calibration .....	23
2.2.4. Electrical Run-out .....	24
2.3. Related Work .....	24
2.4. Conclusions .....	27
2.4.1. Aims and Objectives.....	27
3.0 Sensor Testing & Selection.....	29
3.1. Sensor Specification Requirements.....	29
3.2. Laser Triangulation Testing .....	31
3.2.1. Warm Up Period Test .....	32

3.2.2.	Thermal Stability Test.....	34
3.2.3.	Static Resolution Test.....	36
3.2.4.	Dynamic Resolution Test.....	37
3.2.5.	Conclusions of Laser Testing .....	39
3.3.	Eddy Current Testing.....	40
3.3.1.	Thermal Stability .....	40
3.3.2.	Linearity and Calibration .....	45
3.3.3.	Sensor Sensitivity Test.....	46
3.3.4.	Static Resolution Test.....	47
3.3.5.	Dynamic Resolution Test.....	48
3.3.6.	Conclusions of Eddy Current Sensor Testing .....	50
3.4.	Capacitance Sensor Testing.....	51
3.5.	Non-Contact Sensor Solution .....	52
4.0	System Design .....	57
4.1.	Equipment Design .....	57
4.1.1.	Test-bar Design .....	57
4.1.2.	Fixture Design .....	60
4.1.3.	Data Acquisition .....	61
4.2.	Data Processing.....	63
4.2.1.	Thermal Data Processing.....	63
4.2.2.	Geometric Data Processing .....	65
4.2.2.1.	Donaldson reversal method .....	66
4.2.3.	Vibration Data Processing .....	68
4.3.	Chapter Conclusions.....	70
5.0	Practical Spindle Analysis .....	71
5.1.	In situ Calibration .....	71
5.2.	Thermal Analysis .....	72
5.2.1.	Thermal Imaging .....	74
5.3.	Geometric Analysis .....	75
5.4.	Vibration Analysis.....	78
6.0	Conclusions .....	79
7.0	Future Work.....	80
7.1.	Test-bar Design and Holding .....	80
7.2.	Fixtures .....	81

7.3.	Data Processing Software .....	82
7.4.	Test Methodology .....	82
8.0	References .....	83
9.0	Appendix.....	86
9.1.	Micro Epsilon Eddy Current Testing .....	87
9.2.	Further Examples of Practical Spindle Analysis .....	89

## Table of Figures

---

Figure 1.1 – Sectional View of a motorised spindle [1] .....	12
Figure 1.2 – Geometric Spindle Errors [3] .....	13
Figure 2.1 – Typical setup for ETVE or Spindle Heating Test [2] .....	17
Figure 2.2 – Five-sensor system for measurement of rotating sensitive direction spindle error motions [3] .....	18
Figure 2.3 – Error motion polar plot displaying synchronous and asynchronous error motion [3].....	18
Figure 2.4 – Principle of capacitance sensor [5] .....	20
Figure 2.5 – Laser triangulation principle [38] .....	21
Figure 2.6 – Principle of eddy current sensor [7] .....	22
Figure 3.1 – Thermal Warm up Test Setup.....	32
Figure 3.2 – 15 min Warm Test with Aluminium Fixture.....	33
Figure 3.3 – 15 min Warm Up Test with Carbon Fibre Fixture .....	33
Figure 3.4 – Thermal Image Showing Spot Positions .....	34
Figure 3.5 – Plot of Spot Temperatures .....	35
Figure 3.6 – Displacement during 2 hour stability test .....	35
Figure 3.7 – Static resolution test setup .....	36
Figure 3.8 – Static resolution with 0 x averaging displacement data .....	36
Figure 3.9 – Static resolution with 16 x averaging displacement data .....	37
Figure 3.10 – Dynamic resolution test setup .....	38
Figure 3.11 – Dynamic resolution with 0 x averaging displacement data .....	38
Figure 3.12 – Kaman eddy current sensor and signal conditioning unit .....	40
Figure 3.13 – Thermal stability test setup.....	41
Figure 3.14 – Comparison of displacement and temperature during thermal stability test .....	41
Figure 3.15 – Comparison of displacement and temperature during second thermal stability test ...	42
Figure 3.16 – Sensor 2 temperature against displacement.....	43
Figure 3.17 – Sensor 3 temperature against displacement.....	43
Figure 3.18 – 50 hour thermal stability test.....	44
Figure 3.19 – Non-linear output from eddy current sensor .....	45
Figure 3.20 – Repeatability results for eddy current sensor output .....	46
Figure 3.21 – Repeatability results for eddy current sensor output .....	46



Figure 3.22 – Eddy current static resolution test setup .....	47
Figure 3.23 – Eddy current static resolution .....	48
Figure 3.24 – High resolution piezo platform dynamic resolution test setup .....	49
Figure 3.25 – Renishaw XL80 laser output on vibration rig .....	49
Figure 3.26 – Output from eddy current sensor on vibration rig .....	50
Figure 4.1 – Manufacture of short aluminium test-bar .....	58
Figure 4.2 – Short Test-bar measuring radial error motion .....	58
Figure 4.3 – Long Test-bar measuring tilt error motion .....	59
Figure 4.4 – Adjustable fixture of radial error motion testing .....	60
Figure 4.5 – Invar fixture for thermal testing .....	61
Figure 4.6 – National Instruments data acquisition device .....	62
Figure 4.7 – Raw thermal data plot converted to microns .....	63
Figure 4.8 – Post possessing averaged data plot .....	64
Figure 4.9 – Surface mountable temperature sensor .....	64
Figure 4.10 – Temperature data .....	65
Figure 4.11 – Donaldson reversal technique [20] .....	66
Figure 4.12 – Peak finding data .....	67
Figure 4.13 – Peak finding data .....	68
Figure 4.14 – FFT plot of spindle vibration in the Z-Axis direction when rotating at 1000rpm .....	69
Figure 4.15 – Zoomed in FFT plot of spindle vibration in the Z-Axis direction when rotating at 1000rpm .....	69
Figure 5.1 – Spindle displacement during a 6 hour spindle heating test .....	72
Figure 5.2 – Spindle temperature during a 6 hour spindle heating test .....	73
Figure 5.3 – Comparison of temperature and displacement during a 6 hour spindle heating test .....	73
Figure 5.4 – Thermal imaging at various times of a heating and cooling test .....	74
Figure 5.5 – All run plotted from run 1 .....	75
Figure 5.6 – All runs plotted from run 2 .....	76
Figure 5.7 – All runs plotted in a polar plot .....	76
Figure 5.8 – Averaged data run-out plot .....	77
Figure 5.9 – Vibration data from an air bearing spindle running at 250rpm .....	78
Figure 5.10 – Vibration data from an air bearing spindle running at 500rpm .....	78
Figure 7.1 – Adjustable tool holder to 0.000 $\mu$ m run-out [39] .....	80
Figure 7.2 – Ultrafine adjustment screws [40] .....	81
Figure 9.1 – Linearity of Micro-Epsilon eddy current sensor .....	87

Figure 9.2 – Stability of Micro-Epsilon eddy current sensor .....	88
Figure 9.3 – Thermal step heating test displacement measurement.....	89
Figure 9.4 – Thermal step heating test temperature measurement.....	90
Figure 9.5 – Thermal step heating test thermal imaging .....	90
Figure 9.6 – Thermal step heating test temperature and displacement comparison .....	91
Figure 9.7 – Radial run-out of ball bearing spindle at 1000rpm .....	92
Figure 9.8 – Tilt error of ball bearing spindle at 1000rpm.....	92
Figure 9.9 – Vibration of ball bearing spindle at 1000rpm .....	93

## Table of Tables

---

Table 1 - Minimum Required Specification .....	30
Table 2 - Keyence Laser Specification .....	31
Table 3 – Comparison of Non-Contact Measurement Sensors Part 1 .....	53
Table 4 - Comparison of Non-Contact Measurement Sensors Part 2.....	54
Table 5 – Advantages and Disadvantages of the Potential Systems .....	55
Table 6 – Spindle Analysis B.O.M.....	70
Table 7 – Potential Resolutions at various positions in the sensor range .....	88

## 1.0 Introduction

---

The precision engineering industries demand for high volume automated production has led to the continuing development of CNC machine tools. Over the years, machine tool and spindle manufacturers have been faced with the challenge of producing faster and higher accuracy equipment to cope with the industries continuous improvement ethos.

It is the primary goal of machine tool manufacturers and maintenance teams to bring their machine tools in to a state where they can consistently produce parts to within a specified tolerance. Within manufacturing, especially the aerospace industry, part tolerances have tightened considerably over recent years. These tight tolerances require high levels of repeatability and accuracy from the machine tools and spindles used to produce these parts.

The ability to produce accurate components has many advantages, with some of the most important being:

- A reduction in the costs incurred by remanufacturing or scrapping out of tolerance components
- Tolerances can be reduced allowing the production of more accurate assemblies
- An increased possibility of a part being both roughed and finished on the same machine, resulting in reduced setup time
- More accurate parts being produced, leading to improved efficiency e.g. in engines and compressors

While understanding machine tool errors is a large and complex subject and should not be understated, spindle error measurement is becoming increasingly important to machine tool users in high precision manufacturing, as they look to characterise their spindle performance capabilities.

Historically, machine tool spindles were driven by gear or belt systems, with the speed only variable by a transmission. The requirement from industry for increased productivity led to the development of new bearings, power electronics, inverter systems and low cost 3 phase motors, which in turn led to the production of high speed motorised spindles.

Today, the majority of machine tools are equipped with these motorised spindles [1]. This reduces the number of moving parts and the potential for unwanted vibration from mechanical transmission elements like gears and couplings.

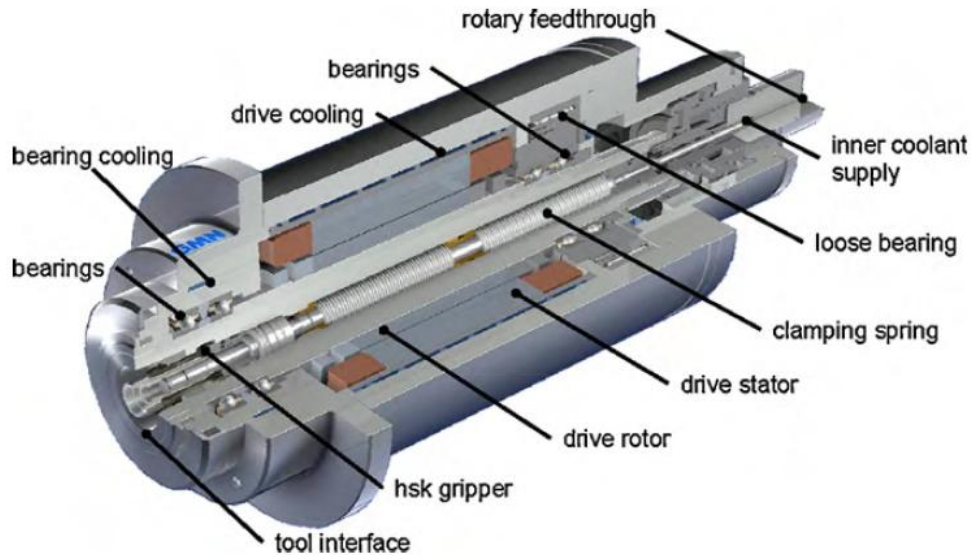


Figure 1.1 – Sectional View of a motorised spindle [1]

Figure 1.1 shows a typical configuration of a motorised machine tool spindle, with all the individual elements identified.

The spindles have at a minimum of two sets of bearings; predominantly ball bearings are used although air bearings are becoming more popular in very high precision operations. The bearing system is the component with the greatest influence on the lifetime of a spindle, so periodic monitoring of bearing condition is advisable.

Due to high power outputs of the motor and high rotational speeds, active cooling is often required. This is generally implemented through water based cooling. The coolant flows through a cooling sleeve around the stator of the motor and often the outer bearing rings.

Seals at the tool end of the spindle prevent the intrusion of swarf and coolant; this is often achieved with purge air and a labyrinth seal. A standardized tool interface such as HSK or SK is utilised at the spindles front end with a clamping system for fast automatic tool changes.

Spindle errors typically account for up to 30% of overall machine tool errors, and catastrophic spindle failures bring production to a standstill, until a new spindle can be fitted. At worst case this can result in several weeks downtime waiting for a new spindle, or companies holding expensive spares (replacement spindles typically cost between £20k and £50k). Based on the past records of a well known British manufacturer, spindle failure is a significant factor affecting machine availability, it is important to understand their errors and point of failure, to be able to predict maintenance requirements.

## 1.1. Spindle Error Sources

As previously mentioned, high volume, tight tolerance components are now the norm in industry. These tight tolerances require high levels of repeatability and accuracy from the machine tools and spindles used to produce them. The sources of error responsible for affecting these spindle performance parameters can be split into three main areas:

- Geometric errors
- Non-rigid errors
- Thermal errors

### 1.1.1. Geometric Spindle Errors

As the spindle rotates about its axis, any deviation from the true axis of rotation will result in a geometric spindle error. This could be a radial error in the X and Y directions, an axial error in the Z direction or a tilt error in the X and Y directions (see figure 1.2).

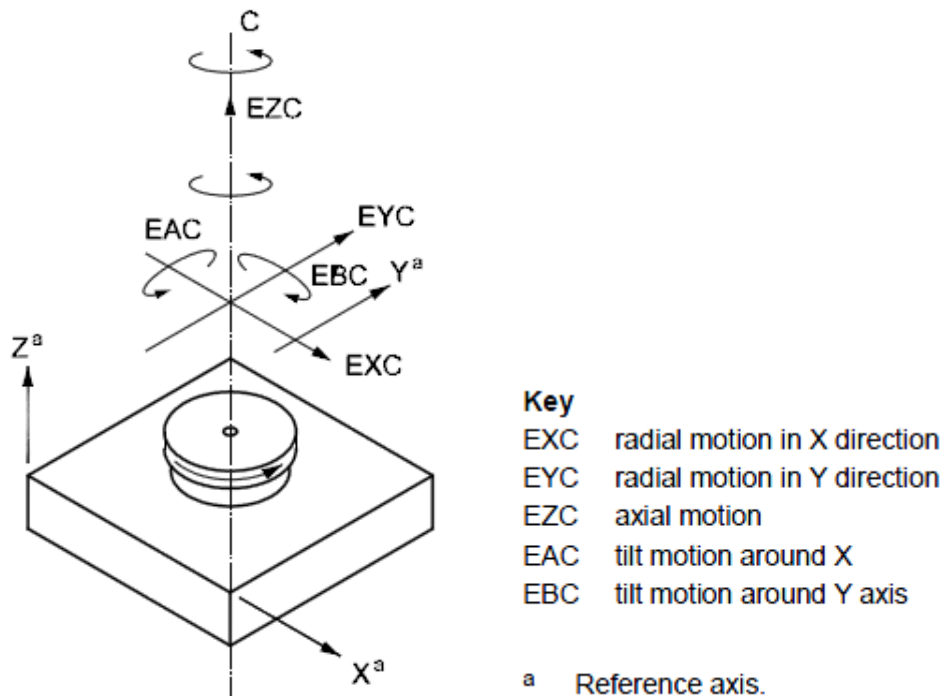


Figure 1.2 – Geometric Spindle Errors [3]

These errors occur as a result of small mechanical imperfections and misalignment of the spindle assemblies. The magnitude of these errors is dependent on the quality of the manufacturing process. Despite the majority of spindle manufactures being able to minimise these errors through good

design and careful assembly, some level of inherent error will remain. In addition, continued use of the spindle will result in bearing wear and degradation of the overall bearing condition over time. This will increase the magnitude of the error and will eventually lead to spindle failure.

### **1.1.2. Non-Rigid Spindle Errors**

Non-rigid errors also known as load induced errors result from factors such as spindle inertia and cutting forces. It could be induced from any moving part within the spindle, i.e. bearings, races, shaft. These errors vary with speed and dependant on magnitude can cause a poor quality surface finish on manufactured parts.

Sources of these errors resulting in poor surface finish could include:

- An out of balance shaft, which would produce a once per revolution error
- A damaged ball bearing, which would produce an asynchronous error at the ball rotation frequency
- Damaged bearing races, which again would produce an asynchronous error at the ball pass frequency

When cutting in a sensitive direction, these errors will result in a one for one error on the part at the magnitude of the induced vibration.

### **1.1.3. Spindle Thermal Errors**

Thermally induced errors occur due to changes in temperature of the spindle and surrounding structure. These can be categorised into internally and externally generated.

Internally generated heat is produced from the moving elements within the spindle such as, bearings, motors and gears where high friction causes a temperature increase of the components. This generated heat will flow through the spindle and machine structure causing thermal expansion and resulting in distortion between tool and work-piece. This distortion could vary dependant on processes being carried out, for example processes requiring a high spindle speed will induce more heat and therefore a larger error.

Externally generated heat is produced from changes in temperature around the machine. This could be from an environmental temperature fluctuation throughout the course of the day, the opening and closing of workshop doors, a workshop heating system or heat generated by other machines in close vicinity.

## **1.2. Chapter Conclusions**

A demand for tighter tolerances and faster process times in the manufacturing industry has resulted in the requirement for extremely accurate and high speed spindles. This has led to machine tool users having a requirement to quantify spindle errors so that they can assess their capability for producing components to specification. The sources of error affecting spindle performance are:

- Geometric errors
- Non-rigid errors
- Thermal errors

This has led to the investigative work described in this report, into the most significant static and dynamic errors associated with a variety of common machine tool spindles. Also, the development of robust non-contact measurement hardware and analysis methods for efficient characterisation of these errors.

Surprisingly, there are but a few commercial systems available on the market that are capable of analysing spindle errors on precision machine tools. However, the systems use capacitance sensing technology, which may not always be suitable for use in a manufacturing environment. The systems are also very expensive and so may not be a viable option or at least difficult to budget for the majority of small to medium size enterprises (SME's). Another potential problem is that a single system may not have sufficient sensitivity or range to measure both geometric and thermal errors on a range of spindles potentially present in such factories. Section 2 includes a review of the specifications of some existing systems.

The desired solution is a spindle analysis system that is capable of being taken to customer sites by service organisations or utilised by maintenance teams, to perform spindle analysis testing on their machine tool spindles in all types of manufacturing environments.



## **2.0 Literature Review**

---

As mentioned in the introduction, a demand for tighter tolerances and faster processing times in the manufacturing industry has resulted in the need for extremely accurate and high speed spindles. The requirement of the machine tool manufactures and maintenance teams to measure and quantify the inherent errors present in these spindles has resulted in the production of a series of international standards.

### **2.1. ISO Standards**

These standards have been prepared by a technical committee with the aim to standardise test methods for determining spindle errors. The standards relevant to spindle analysis Include:

- ISO 230 part 3 - Determination of thermal affects
- ISO 230 part 7 - Geometric accuracy of axes of rotation
- ISO 230 part 8 - Determination of vibration levels

#### **2.1.1. Determination of Thermal Affects**

ISO 230 part 3 ‘Determination of Thermal Affects’ is the standard for assessing internal and external thermal influences on machine tool and spindle behaviour. The standard describes three main tests:

- Environmental Temperature Variation Error (ETVE) test
- Thermal Distortion Caused by Rotating Spindle test (spindle heating test)
- Thermal Distortion Caused by Linear Motion of Components test (axis heating test)

An ETVE test can be performed to assess the effect of environmental temperature changes on the machines positional accuracy. A spindle heating test can be conducted to identify the effects of the internally heat generated by rotation of the spindle(s) and the resultant temperature gradient along the structure and the distortion of the structure observed between the work-piece and the tool. An axis heating test can be carried out to identify the effects of internal heat generated by the driving system components, such as the ball-screw, nut and support bearings, on the distortion of the machine tool structure observed between the work-piece and the tool. [2]

The standard suggests using non contact measurement sensors to measure the linear and angular displacement of the spindle relative to the work-piece as it rotates, while monitoring the temperature of the machine structure near the spindle nose, the machine ambient temperature and the spindle ambient temperature. An example setup used in the ISO standard can be seen in figure 2.1.

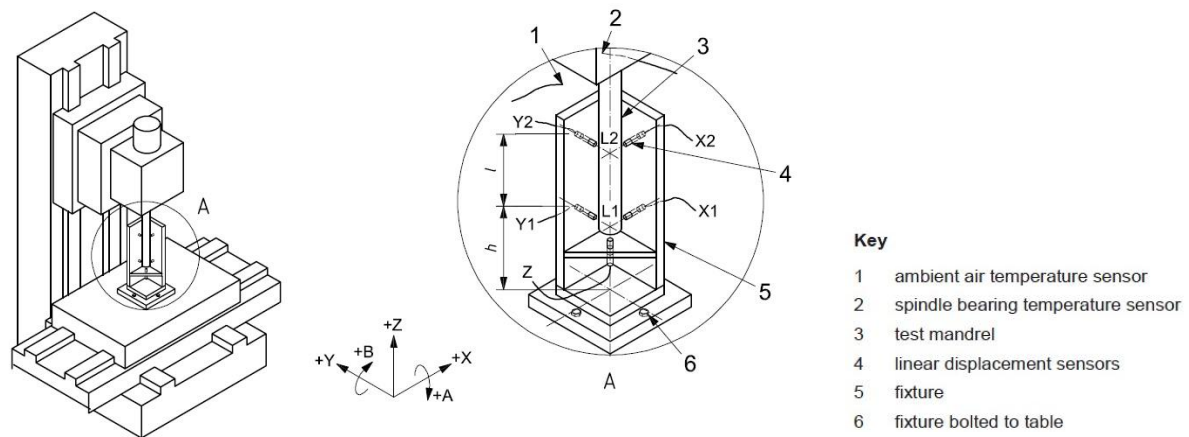


**Figure 2.1 – Typical setup for ETVE or Spindle Heating Test [2]**

Non-contact measurement sensors are recommended for thermal testing however, many machine tool users and service teams don't have access to this type of technology and so may use indicator clocks or other contact probe method. This involves a simple routine that measures the displacement of the spindle relative to the work piece, usually performed every 15 minutes, and requires the spindle to be stopped in order to take the measurement. This method is not very accurate and can result in poor thermal profiling of a machine.

### **2.1.2. Geometric Accuracy of Axes of Rotation**

ISO 230 part 7 'Geometric Accuracy of Axes of Rotation' is the standard for assessing the accuracy of machine tool spindles, rotary heads and rotary / swivelling tables. The standard describes tests for two machine configurations, rotating sensitive direction and fixed sensitive direction. For each of these there are three tests to measure the geometric error:

- Radial Error Motion
- Axial Error Motion
- Tilt Error Motion

For all three of these tests, the standard suggests using non contact measurement sensors to measure the displacement of the spindle relative to the work-piece as it rotates. An example setup used in the ISO standard can be seen in figure 2.2.

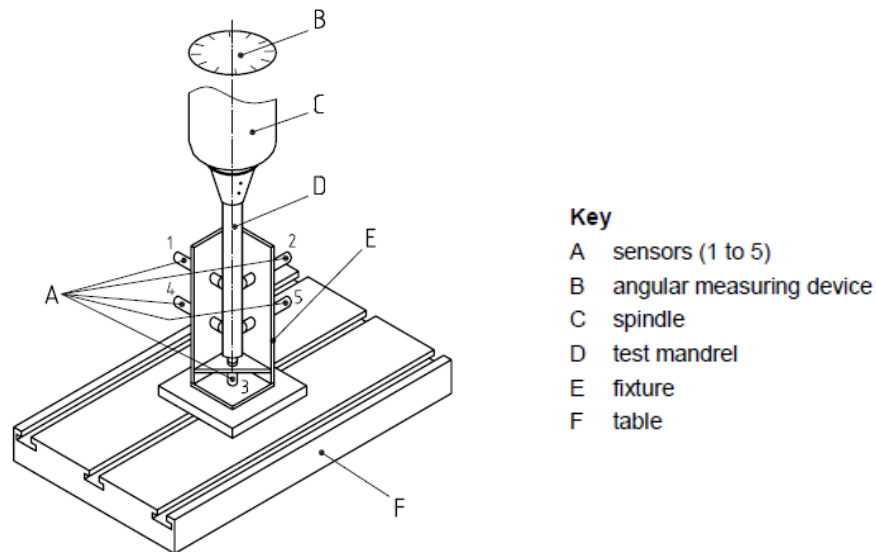


Figure 2.2 – Five-sensor system for measurement of rotating sensitive direction spindle error motions [3]

The output from radial and axial error motion tests are two error motion values, calculated from the error motion polar plot. These are the synchronous error motion value, errors that occur at the same frequency as the rotational speed of the spindle (once per revolution errors) and the asynchronous error motion value, errors that occur at frequencies other than the rotational speed of the spindle. Figure 2.3 shows a typical polar plot and displays the points of maximum synchronous and asynchronous error motion.

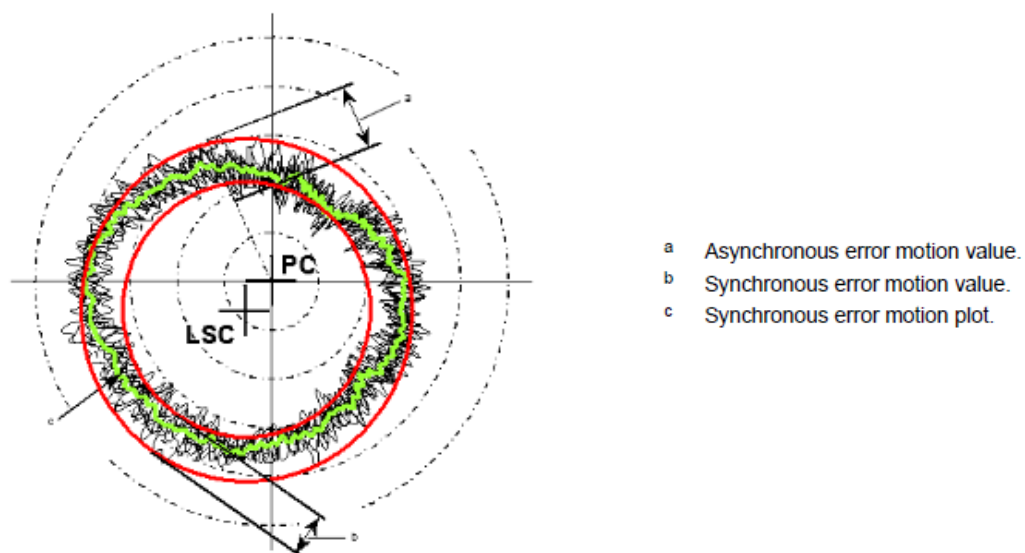


Figure 2.3 – Error motion polar plot displaying synchronous and asynchronous error motion [3]

### **2.1.3. Determination of Vibration Levels**

ISO 230 part 8 'Determination of Vibration Levels' is the standard for assessing the affect of vibration on work-piece accuracy and surface finish quality. The requirement for vibration control is recognised through the manufacturing industry so that vibration causing undesirable effects can be mitigated. These effects are identified principally as: [4]

- unacceptable cutting performance with regard to surface finish and accuracy
- premature wear or damage of machine components
- reduced tool life
- unacceptable noise level
- physiological harm to operators

Only vibration errors that occur as a result of unacceptable cutting performance are covered in the scope of ISO 230. It is these errors that are investigated during spindle analysis.

This part of the ISO 230 standards is in the form of a technical report and as such does not describe standard methods of test for identifying unwanted vibration magnitudes.

### **2.1.4. ISO Standards Conclusions**

The tests described above from the ISO standards all require the machine to be freed up to allow testing to take place. When faced with the types of production targets talked about previously, production teams are apprehensive about taking a machine off line to perform capability testing. A system with a standard setup that could be used to measure all spindle error would be extremely advantageous in terms of reduced setup time of equipment and testing times. The standard doesn't specify a type or make of instrumentation to be used to carry out testing, so it is left to the user to find a solution. It is not likely that this solution will comprise of a single piece of equipment and based on the limited number available, capable of dynamic measurement, it will most likely be expensive and sometimes prohibitively so. The alternative is to use a service provider but similar issues may occur if lots of measurements are required, for example for lots of machines and/or for statistical process control (SPC) or preventative maintenance.

## 2.2. Non-Contact Sensing Technology

The aforementioned standards suggest the use of non contact measurement to analyse the spindle behaviour. The ability to monitor a target without physical contact offers several advantages over contact measurement, including the ability to achieve higher measurement resolution and increased dynamic response to moving targets. They are also virtually free of hysteresis and there is limited risk of damaging fragile targets because of contact with a measurement probe. Three typical non contact measurement sensing technologies (as suggested by ISO) are [2] [3]:

- Capacitance
- Eddy Current
- Laser triangulation

Each of these technologies has its advantages and disadvantages for use in spindle analysis. The following sections look at these sensors in detail and describes there suitability for use in spindle analysis measurement.

### 2.2.1. Capacitance Sensors

Capacitive sensors work by measuring changes in an electrical property called capacitance. Capacitance describes how two conductive objects with a space between them respond to a voltage difference applied to them. When a voltage is applied to the conductors, an electric field is created between them causing positive and negative charges to collect on each object (see figure 2.4). If the polarity of the voltage is reversed, the charges will also reverse.

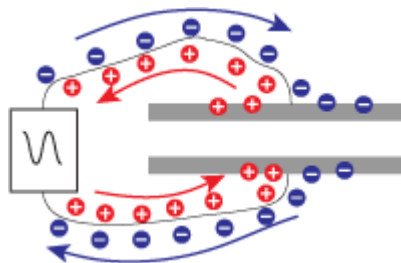


Figure 2.4 – Principle of capacitance sensor [5]

Capacitive sensors use an alternating voltage which causes the charges to continually reverse their positions. The moving of the charges creates an alternating electric current which is detected by the sensor. The amount of current flow is determined by the capacitance, and the capacitance is

determined by the area and proximity of the conductive objects. Larger and closer objects cause greater current than smaller and more distant objects. The capacitance is also affected by the type of nonconductive material in the gap between the objects.

Capacitance sensors can achieve nanometre resolutions with high accuracy measurement and are not sensitive to material changes. However, they are very sensitive to changes in the interfacial fluid i.e. they are affected by dirty environments where dust, oil and coolant may be present between the sensor and the measuring surface.

### 2.2.1. Laser Triangulation Sensors

Laser triangulation sensors work by emitting a laser beam onto a target and reflecting it back onto a detector in a triangular configuration. The laser beam is projected through a lens to the target and is then reflected from a target surface to a collection lens. This lens is typically located adjacent to the laser emitter. The lens focuses an image of the spot on a linear array camera. The camera views the measurement range from an angle that varies from 45 to 65 degrees at the centre of the measurement range. The position of the spot image on the pixels of the camera is then processed to determine the distance to the target as in figure 2.5.

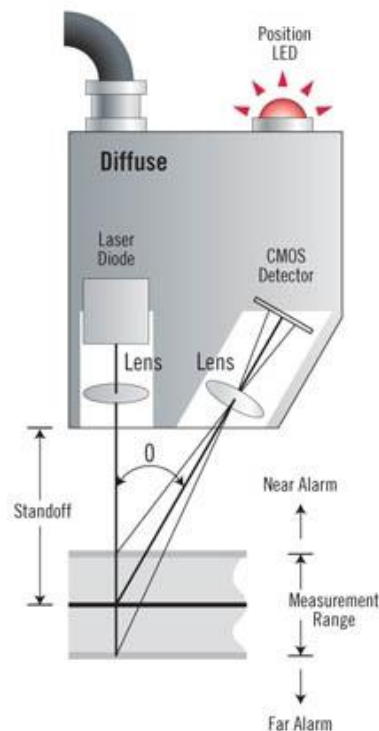


Figure 2.5 – Laser triangulation principle [38]

The signal from the detector is used to determine the relative distance to the target. This information is then typically available through an analog output, a digital interface or a digital display for processing.

Laser triangulation sensors have a large standoff so there is a reduced risk of damage during setup and also offer very high sampling frequencies. However, they are susceptible to self heating, environmental influences such as humidity and material in the gap between the sensor and the target. They are also quite bulky and expensive.

### **2.2.2. Eddy Current Sensors**

Eddy current sensors operate on a principle based on Lenz's law [6]. Most eddy current sensors are constructed with a sensing coil, which is a coil of wire in the head of the probe. When an alternating current is passed through the coil it creates an alternating magnetic field. When a metallic target is present in this magnetic field the electromagnetic induction causes an eddy current in the target material in a perpendicular plane to the magnetic field of direction. This induced eddy current generates an opposing magnetic field which resists the field generated by the sensing coil. The interaction of the two magnetic fields is sensed using electronics and converted into an output voltage that is directly proportional to the distance between the sensor and the target.

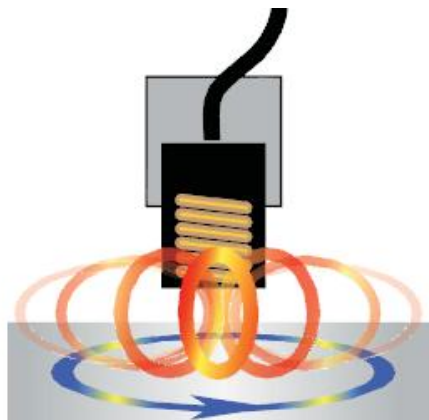


Figure 2.6 – Principle of eddy current sensor [7]

Compared to the other noncontact sensing technologies, high-performance eddy-current sensors have some distinct advantages.

- Tolerance of dirty environments
- Not sensitive to the interfacial material between the probe and target
- Often less expensive and much smaller than laser triangulation devices
- Often less expensive than capacitive sensors

Eddy current sensors are not without their disadvantages. The main challenge is that the output changes with the use of different target materials. This leads to a requirement for careful calibration of the sensors.

### **2.2.3. Eddy Current Sensor Calibration**

It is normal practice that the eddy current sensors are calibrated by the manufacturer before they are delivered to the customer [8]. Each sensor is calibrated to its own individual signal conditioning unit; these cannot be interchanged between sensors without affecting the output. The length of cable used to connect the sensor to the signal conditioning unit also has an effect on the output, so once calibrated cannot be exchanged for a cable of differing length. The main challenge for high-end specification eddy current sensors with linear outputs in the region of 0.2% is that they must be calibrated to a specific target material. There is a significant difference in the output of the sensors when used with a ferrous target compared to a non-ferrous target and as such the sensors are usually calibrated to either one or the other.

This leaves room for a certain amount of measurement uncertainty between materials of a similar nature. For example the output from an aluminium alloy target would be different to that of pure aluminium. Some sensor manufactures provide a method for self calibration for fine adjustment [8]. However, if it is necessary to use the sensors on both ferrous and non-ferrous target then either a new set of sensors will be required or they will continuously need to be sent back to the manufacturer for re-calibration to a new target material.

Alternatively low cost eddy current sensors are available that are not calibrated to a specific target material. However, the output from these sensors can be very non-linear and as such requires careful calibration (see section 3.3.2 for details on calibration methods).



#### **2.2.4. Electrical Run-out**

A further concern when using eddy current sensors is the occurrence of a phenomenon known as electrical run-out. As described by Yating [9], the electrical run-out problem is caused by the change or uneven distribution of sample conductivity and relative permeability of the target material. As eddy current sensors work by penetrating the surface of a target when creating a magnetic field, any defects that appear under the surface will affect the reciprocated magnetic field and hence the voltage, which is used to determine the distance between the sensor and the target. The penetration depth of the magnetic field depends on the permeability of the target material. Teruhiro & Ma [10] [11] look at the permeability of a number of metal composite materials. The affects of this problem and methods used to mitigate it are explored in later chapters.

### **2.3. Related Work**

In order to gain an understanding spindle error it is important to understand spindle design and the latest technologies being employed. The CIRP Annals 2010 [1] investigates the latest in machine tool spindle units, providing detailed information about spindle components and there thermal and dynamic behaviour. The majority of machine tools in use today are equipped with motorised spindles to enable higher speeds to be achieved and reduce the number of mechanical parts with the potential to fail.

These spindles have a minimum of two bearing sets, predominately using a ball bearing design and it is this bearing system that has the greatest influence on the lifetime of the spindle. Angular contact ball bearings are most commonly used in high speed spindles due to their low friction properties and ability to withstand external loads in both axial and radial directions. A method of predicting bearing life and as a result spindle life would be extremely beneficial to machine tool users when planning maintenance schedules.

Some of the highest precision spindles are found in grinding machines where high accuracy is necessary during finishing operations. The present internal cylindrical grinding spindles have a run-out requirement of less than 1 $\mu$ m. A submicron resolution would therefore be required from the chosen sensor.

In the past an increase in reliable rotational speed was desired to enable greater metal removal rates. The focus has now shifted to spindles with higher achievable torque up to 15,000rpm. When performing spindle analysis this would result in a requirement for a sensor capable of logging data at a minimum of 15 kHz, to capture 60 points per revolution. The standard doesn't specify a required number of points per revolution, but from experience, anything less than 60 points and measurement accuracy starts to be affected.

This reduction in spindle speed also reduces the level of friction and therefore the heat generated from the bearings and motor. According to Bryan [12], machine tool thermal distortion can account for 70% of the total machining error. Methods for reducing thermally induced error through machine and spindle design can help to minimise this error. Postlethwaite [13] discusses thermal error reduction techniques through design and compensation. The majority of error reduction methods involve large amounts of data being captured and used to apply compensation to a machine. This works well for the machine on which the data was captured however, transferring the technique to other machines can be difficult and time consuming. Methods of compensation and thermal error prediction have been well explored [14] [15] [16].

This is not the only method of error reduction, many solutions exist for the machine tool builder to reduce thermal errors that can be applied at the design stage including; symmetric machine tool structures to allow for a uniformed thermal growth and therefore better prediction of thermal error. Liquid circulation cooling systems, which pump chilled oil, water or other coolant around the moving elements to extract some of the heat generated. Low thermal expansion coefficient materials may be applied if they maintain other key material properties. Where this is not a viable option, the machine can be designed so that the direction of thermal growth is away from the thermal datum so as to limit the affect on tool part accuracy.

According to the ISO standards, geometric spindle measurement can be conducted using a number of types of non-contact measurement sensors. Jywe [18] presents a measurement system using laser diode and a quadrant sensor for measuring the radial error motion of a wide range of machine tool spindles. Due to the high sampling frequency of laser measurement, very high speed spindles can still be measured using this method. However, the achievable resolution is only  $0.7\mu\text{m}$  which would not be sufficient for the majority of spindles in production today.

Castro [19] also presents a method of evaluating spindle errors using laser measurement. However, this method implements a laser interferometer, which enables a high resolution of 1nm to be achieved, while still having the benefits of the high sampling frequency. However, using a laser

interferometer would mean that only one measurement at a time would be possible. This would require longer test periods, which would result in longer machine downtime periods.

Eric Marsh [20] has produced a book on precision spindle metrology, describing concepts and techniques for measuring spindle performance.

When running, the spindle speed will fluctuate by some amount. It is therefore important to synchronise the data with the rotation of the spindle. Many spindles have rotary encoders, but access to the output may be difficult. A method for determining the spindle rotation will therefore be required. Marsh suggests using a slightly eccentric target to provide a once per revolution component to the output data. Using this method will require careful control so as not to introduce vibration from imbalance. Xiaodong [21] [22] presents a new method for characterising radial error motion and discusses the limitations of current spindle motion analysis techniques.

Spindle data will contain a variety of components, occurring at different frequencies. Data acquisition requires a fixed sampling frequency, but there is no guarantee that the spectral content of the measurement will be limited to a range within the sampling frequency. Any frequency content above one half of the sampling rate will be incorrectly sampled as a lower frequency during analog to digital conversion.

In high precision spindles that offer nanometre level error motion, it is important to distinguish between spindle error and the out of roundness of a test-bar. As long as the artefact form and synchronous spindle error are repeatable then reversal methods proposed by Donaldson and Estler or a multi probe method will result in complete separation of test bar form errors and spindle error motion. Marsh reviews the advantages of each in his paper, "A comparison of reversal and multi-probe error separation" [23].

As previously mentioned, asynchronous spindle error caused by bearing defects and out of balance shafts can provide unwanted vibration that results in poor surface finishes and form error of machined parts. Martin [24] discusses the need for precision spindle bearing analysis and proposes methods for analysing these errors.

A major source of vibration in precision high speed machine tool spindles is induced from bearing sets. This can be caused by inherent geometrical errors in the assembly, including out of round bearings or out of balance shaft and stator. It may also be caused due to defects in bearing races and other contact surfaces. The magnitude of potential causes often makes vibration diagnostics a difficult task and when it may result in expensive remedial action may be undertaken, it is important to isolate and identify specific vibration causes. Vafaei [25] investigates the use of spectral analysis

techniques to monitor vibration in high speed machine tool spindles. He proposes the use of an auto-regression moving average (ARMA) as opposed to the traditional Fourier analysis. The ARMA method offers higher frequency resolution due to the averaging method employed and better vibration magnitude estimation. However, this method requires a large quantity of data processing to be carried out.

Felten [26] has produced a guide to understanding and identifying bearing vibration frequencies. It provides details on the defect frequencies, including ball pass, ball spin and fundamental frequencies and how to calculate them based on specific spindle speeds and bearing specifications. Once these frequencies have been calculated it is easier to identify them on the vibration spectra and monitoring the magnitude over time, predict bearing failure. ISO standards also exist for calculating load ratings and predicting bearing life [27] [28].

When performing dimensional metrology it is important to employ robust methods of test to enable confidence of test results. Bell and Flack [29] [30] have produced good practise guides to tackle key issues such as traceability and uncertainty of measurement.

## **2.4. Conclusions**

Spindle analysis is a relatively new concept and as such there has been a limited amount of research conducted around the subject. There are solutions for the measurement procedure and interpretation of the errors that have been standardised but the availability of measuring systems is very limited and in most cases not suitable for measuring all the spindle related errors or have limitations when considering their application as a tool or maintenance engineers working in dirty workshop environments.

### **2.4.1. Aims and Objectives**

The aim of the research described in this work is:

- To research and review the differing types of sensing technologies for their applicability to machine tool spindle error measurement
- To investigate data capture and processing methods with consideration of application in workshop conditions

The main objectives of the research are:

- To investigate differing non-contact sensing technologies for their suitability for spindle analysis
- To design suitable test-bars and fixtures for use in a spindle analysis system
- To develop data processing methods
- To provide a more affordable solution for service organisations and maintenance teams
- To be able to perform spindle analysis in manufacturing environments

## 3.0 Sensor Testing & Selection

---

As stated in the literature review, there are three different types of non-contact sensing technologies recommended in the ISO standards. Testing was carried out on some of these sensors to determine the most suitable solution for the desired application, as defined in section 1.2.

### 3.1. Sensor Specification Requirements

The selection of the most appropriate sensor for the specified job is key to the success of the design. From the point of view of this project the most important factors were:

- Resolution
- Range
- Standoff Distance
- Bandwidth or Sampling Frequency
- Linearity
- Accuracy and Repeatability
- Thermal Stability

**Resolution** – This is the smallest increment of displacement that the sensor can measure, for example when measuring the run-out of a machine tool spindle a resolution of  $0.05\mu\text{m}$  would be sufficient for the vast majority of spindles in production. Sometimes the theoretical resolution is not achievable due to noise, typically electrical noise, which may vary depending on how or where the sensor is used, so this must be considered as well.

**Range** – This is simply the distance over which the sensor produces an output, for example in volts that can then be converted into a displacement measurement. The maximum displacements are seen during spindle thermal testing, and experience suggests that anything over  $500\mu\text{m}$  is uncommon. Therefore, this would be the minimum range requirement of the sensor.

**Standoff** – This is the distance between the sensor and the target before an output is produced. A sensor with a very small standoff will increase the likelihood of it being damaged during test setups.

**Sampling Frequency** – This is defined by the number of samples logged over a certain time, usually 1 second and is measured in hertz. Today's high torque spindles have a maximum spindle speed of around 15,000rpm. If a minimum of 60 samples per revolution are required, so that accuracy of the error measurement is not compromised, then this would require a sampling frequency of 15 kHz.

**Linearity** - In an ideal world the output from any sensor would be perfectly linear and not deviate from a straight line at any point. However, in reality there will be slight deviations from this line which define the system linearity. Typically, linearity is specified as a percentage of the Full Scale Measurement Range (FSR). While linearity is a factor, sensors can be calibrated to minimise the error.

**Accuracy and Repeatability** – the accuracy of a sensor is its ability to provide an output as close to that of the true value as possible and the repeatability is its ability to repeat that output for the same measurement over a number of separate tests.

**Thermal Stability** – is the stability of the sensor output over a period of time when subjected to internal or external sources of heat.

#### **Other factors**

The size of the required target area will vary between sensors. For example, laser sensors have a very small spot size (in the order of  $\varnothing 25\mu\text{m}$ ). This allows small test bars to be used which would allow high rotational speeds when measuring high speed spindles. Conversely, eddy current sensors have a larger target area and therefore require large diameter test-bars to be used.

The cost of the sensors is also a significant factor when choosing a solution, as a minimum of 5 sensors are required. Cost is also an issue when replacing broken or damaged sensors; this is especially relevant when dealing with sensors with very small standoff distances.

**Table 1 - Minimum Required Specification**

Minimum Specification	
Resolution	0.05 $\mu\text{m}$
Range	500 $\mu\text{m}$
Sampling Frequency	15 kHz

Table 1 shows the required specification for the most important criteria of the chosen sensor. Although the other factors mentioned in this section are not present in the table, they are still important. However, it is the criteria in the table that will have the largest influence on the sensor selection.

### 3.2. Laser Triangulation Testing

A number of laser triangulation sensors were researched and investigated, to find the most appropriate solution, with the laser that best matched the required specification being the Keyence LK-H022. The sensor had many features that stood it apart from others available including being approximately 60% of the conventional size, with an impressive specification:

**Table 2 - Keyence Laser Specification**

Specification	
Range	6 mm
Sampling Frequency	392 kHz
Spot Size	Ø25µm
Linearity	±0.02% of range
Repeatability	0.02 µm

The specification did not include the sensor resolution; this needed to be determined during testing. There was a concern that the sensor would generate a substantial amount of heat, which may cause problems when performing thermal tests, this also needed to be quantified during testing. The following tests were conducted to help determine whether or not the sensors were capable of being used to perform spindle analysis tests:

- Warm up period test
- Thermal stability test
- Static resolution test
- Dynamic resolution test



### 3.2.1. Warm Up Period Test

The aim of this test was to assess the affect of internally generated heat from the sensor head and the time taken to stabilise.

The test was carried out by setting up the laser in an aluminium fixture against a thermally stable granite table target (see figure 3.1). The sensor was switched on and left to log the displacement of the sensor, while the temperature of the sensor was monitored using a thermal imaging camera.

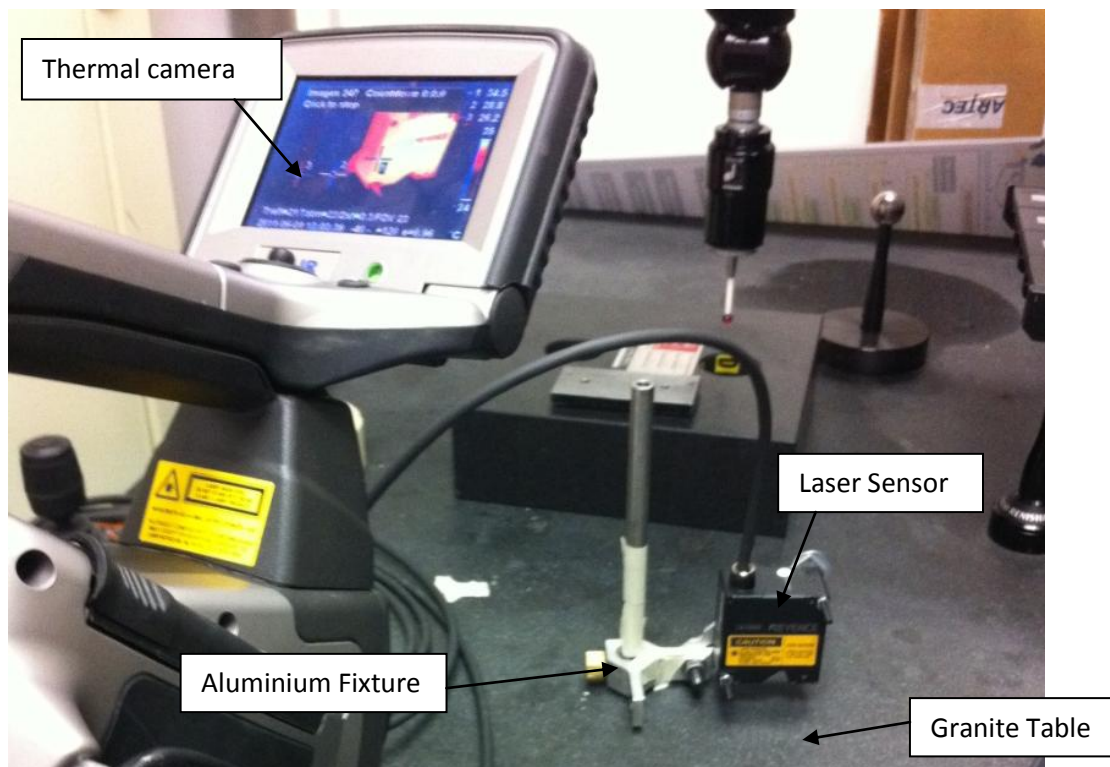
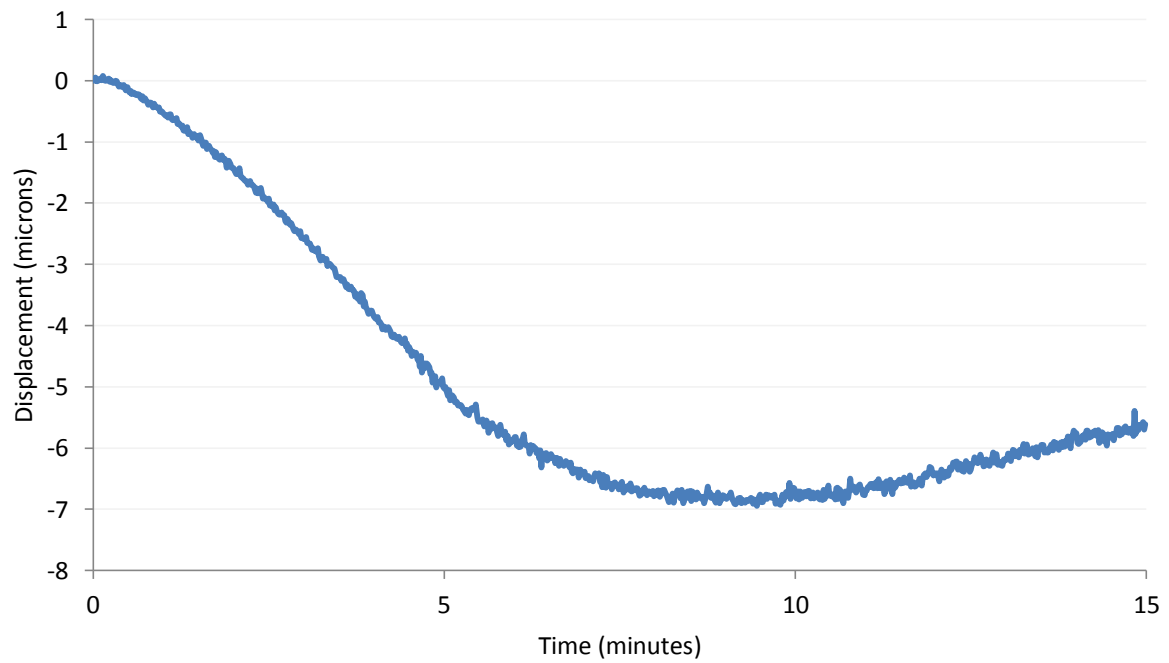


Figure 3.1 – Thermal Warm up Test Setup

The sensor was left logging for 15 minutes, as can be seen in figure 3.2, during which time it displaced by 7  $\mu\text{m}$  before stabilising after approximately 8 minutes.



**Figure 3.2 – 15 min Warm Test with Aluminium Fixture**

The test was then performed again, this time with a carbon fibre fixture, to limit the expansion. As can be seen from figure 3.3, the sensor displaced by 1.5 $\mu$ m before stabilising after approximately 5 minutes.

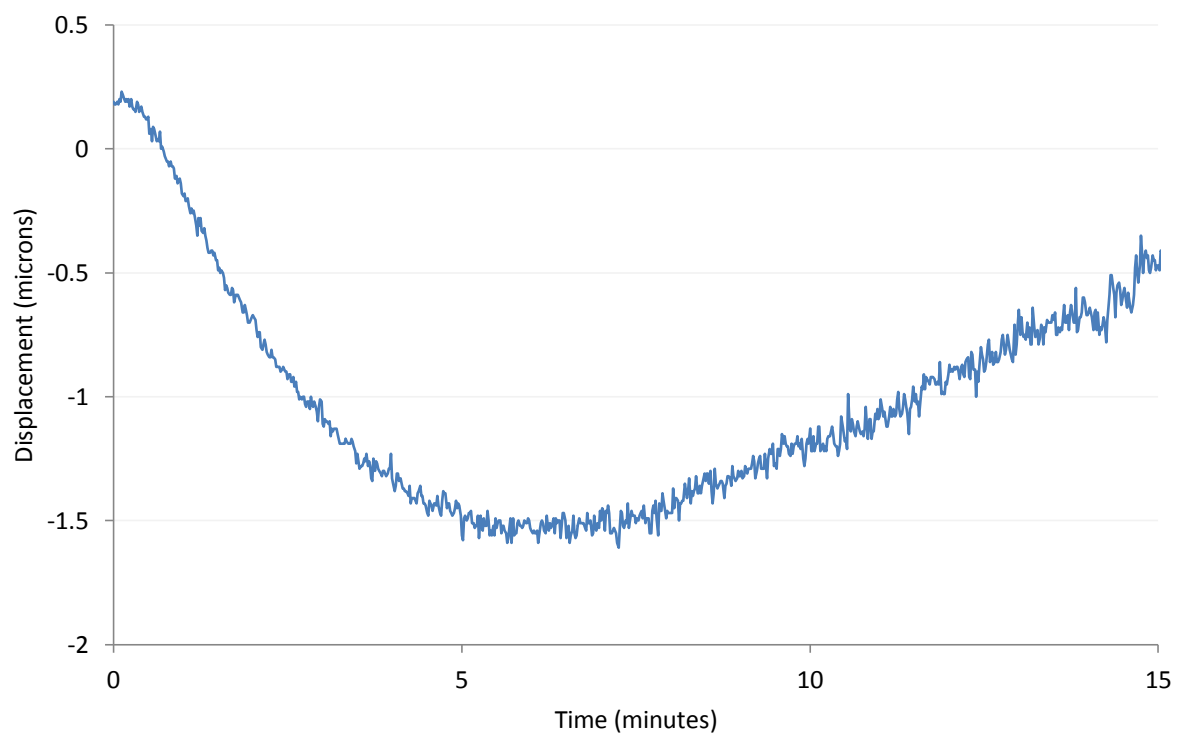


**Figure 3.3 – 15 min Warm Up Test with Carbon Fibre Fixture**

### 3.2.2. Thermal Stability Test

The aim of this test was to assess the stability of the sensor over a longer period of time once the warm up cycle had been carried out.

The test was carried out using the same setup as in the previous test (see figure 3.1) but again using the carbon fibre fixture to limit the thermal growth. The sensor was switched on and left to warm up for the required 5 minutes, the displacement of the sensor was then logged for a two hour duration, while the temperature of the sensor was monitored using a thermal imaging camera. The test was run for 2 hours to give the sensor enough time to be exposed to external sources of heat which could affect the stability of the measurement.

Figure 3.4 shows a thermal image of the sensor and fixture setup with 5 spot positions identified. The temperature at these spots was monitored for the two hour test duration to monitor the flow of heat through the sensor and fixture.

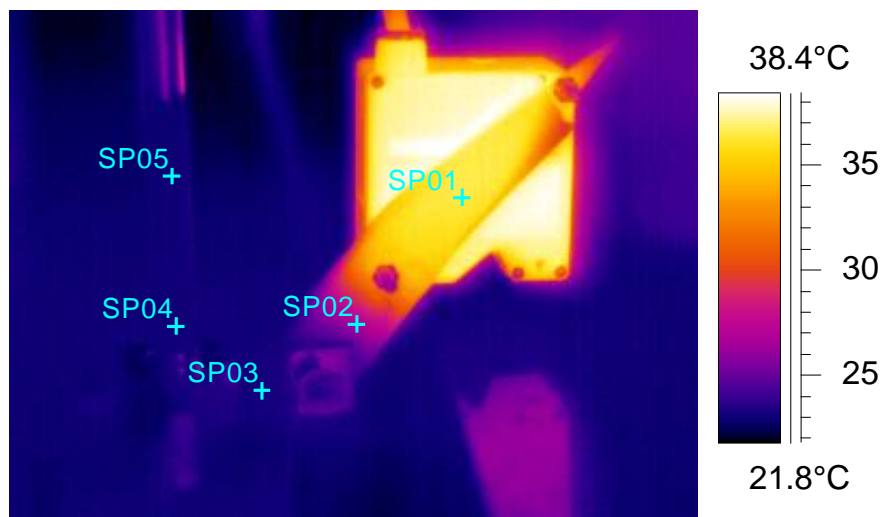


Figure 3.4 – Thermal Image Showing Spot Positions

Figure 3.5 shows the spot temperatures of the sensor and fixture during the two hour thermal stability test. As can be seen from the plot the temperature at each position remained stable to within 0.5 °C for the duration of the test. The sensor itself is very hot, approximately 36.5°C, which may influence tests such as a long term ETVE tests.

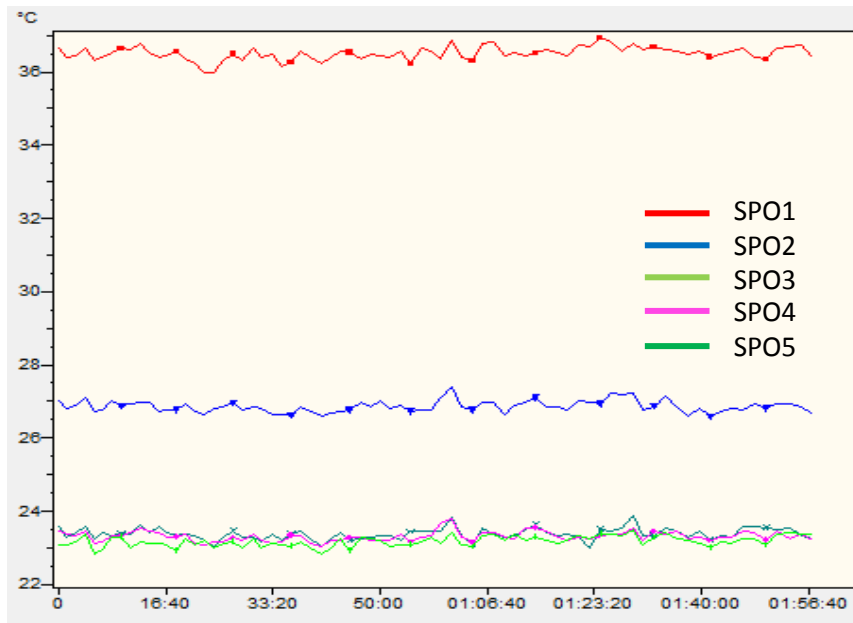


Figure 3.5 – Plot of Spot Temperatures

Figure 3.6 shows the displacement of the sensor during the two hour thermal stability test. As can be seen the displacement is less than  $\pm 0.3\mu\text{m}$ , which is very good for a test of this nature. A displacement of such a small magnitude can be attributed to environmental influence.

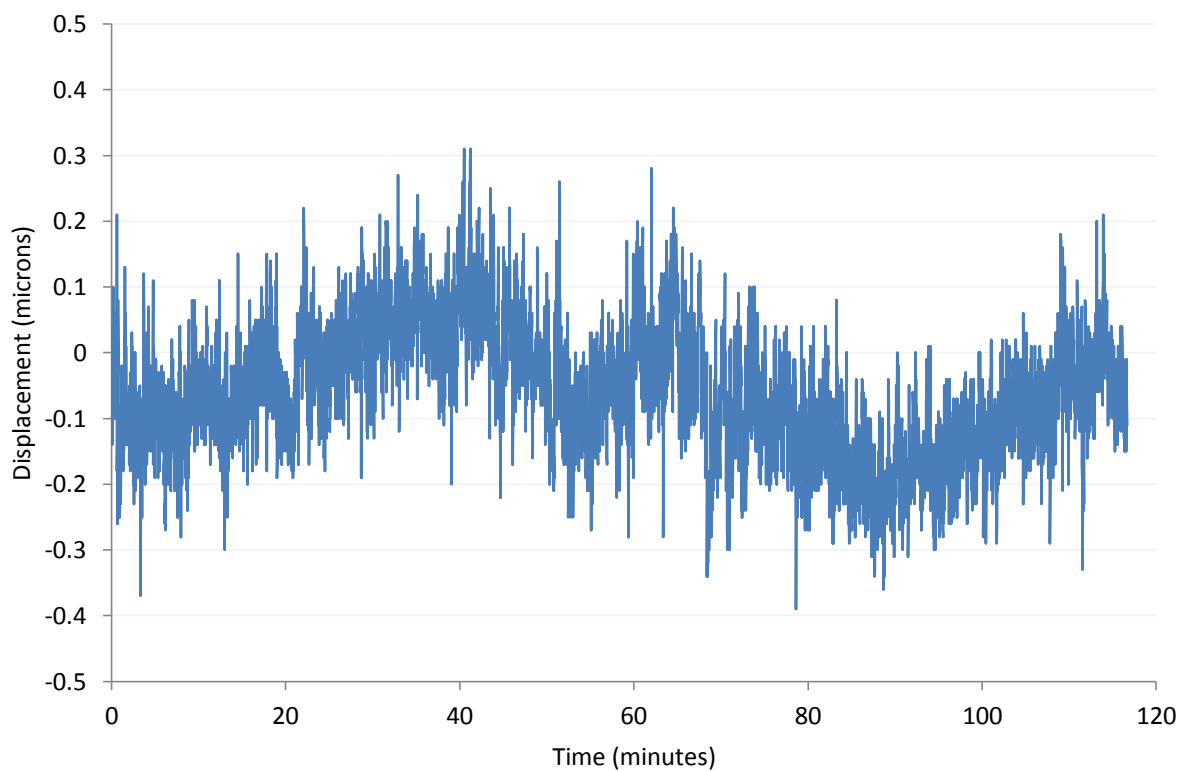


Figure 3.6 – Displacement during 2 hour stability test

### 3.2.3. Static Resolution Test

The aim of this test was to assess the static resolution of the sensor when measuring against a cylindrical test bar, as would be the case during spindle analysis.

The test was carried out by positioning a test-bar against to granite square to limit the influence of any external vibration, as shown in figure 3.7. The sensor was used to log data at the full sampling capability of 392 kHz with no averaging in place.



Figure 3.7 – Static resolution test setup

Figure 3.8 shows the displacement data of the sensor when logging at 392 kHz with no averaging. When logging at such high frequencies there was a lot of noise on the signal, which gives the appearance of the static resolution to be 1  $\mu\text{m}$ .

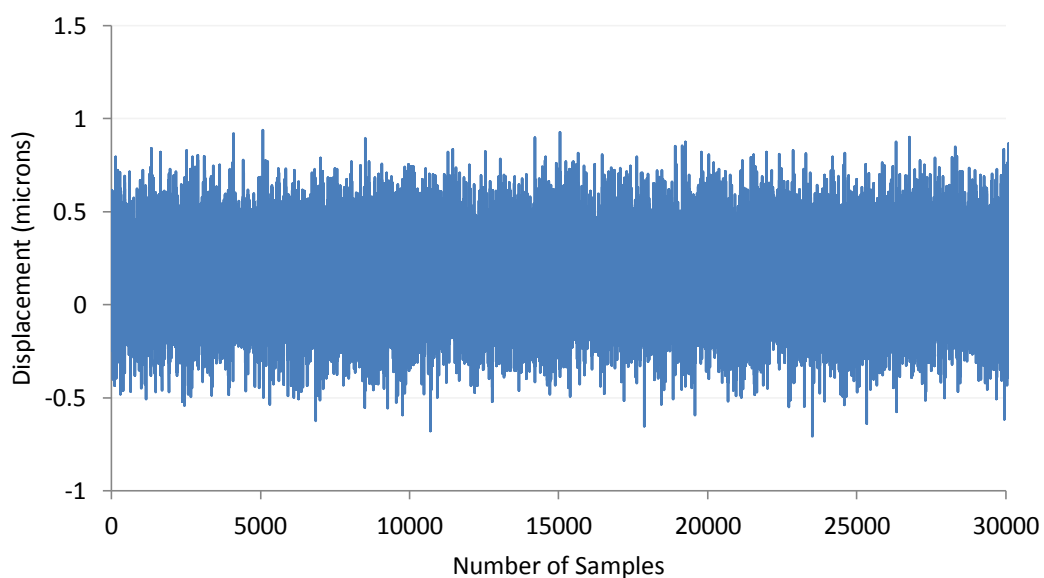
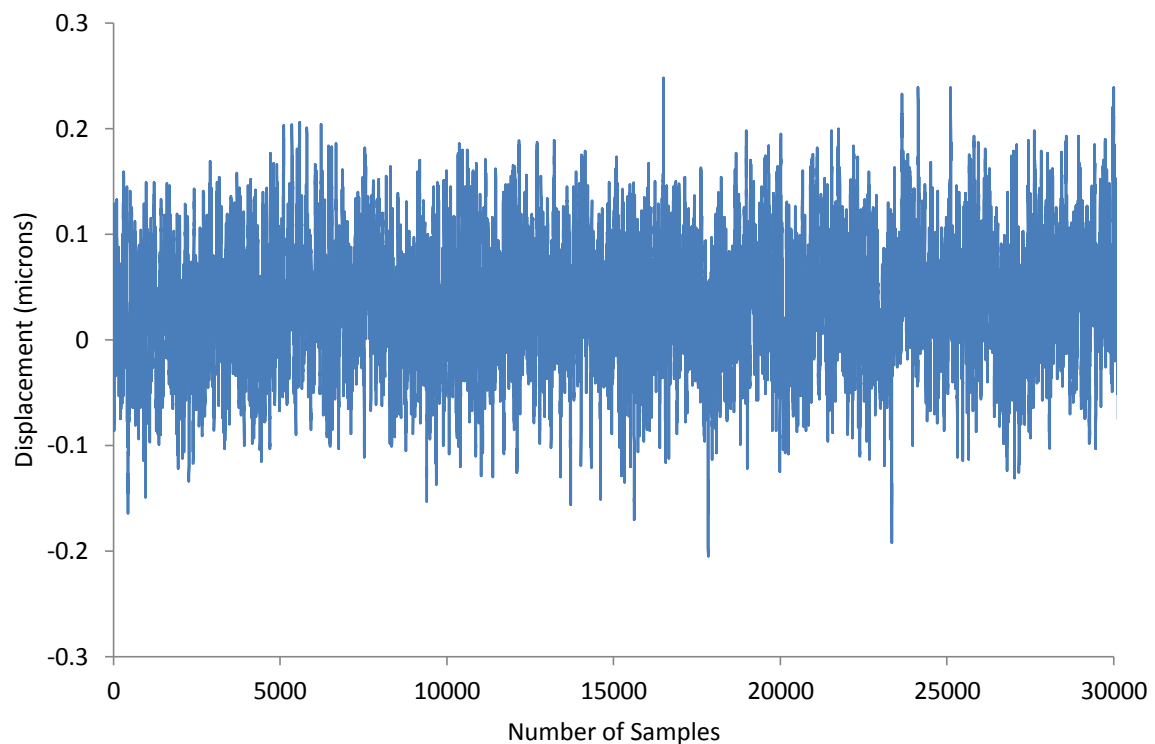


Figure 3.8 – Static resolution with 0 x averaging displacement data

Using standard deviation on the data set to identify the minimum possible signal, measurable with the sensor gives  $0.22\ \mu\text{m}$ . This is quite good; however it exceeds the minimum requirement of  $0.05\ \mu\text{m}$ .

Figure 3.9 shows the displacement data of the sensor when logging at 392 kHz with 16 times averaging. Even with 16 times averaging, this still provides a sampling frequency of 15 kHz, which is in line with other available systems. As can be seen, this reduces the noise on the signal, which gives the appearance of the static resolution to be  $0.3\ \mu\text{m}$ .



**Figure 3.9 – Static resolution with 16 x averaging displacement data**

Using standard deviation on the data set to identify the potential resolution achievable with the sensor, gives  $0.06\ \mu\text{m}$ . This is comparable with the required resolution.

### **3.2.4. Dynamic Resolution Test**

The aim of this test was to assess the dynamic resolution of the sensor when measuring against a cylindrical test bar, as would be the case during spindle analysis.

The test was carried out by positioning a test-bar in a typical machine tool spindle and rotating it at 1000rpm, as can be seen figure 3.10. The sensor was used to log data at the full sampling capability of 392 kHz with no averaging in place.

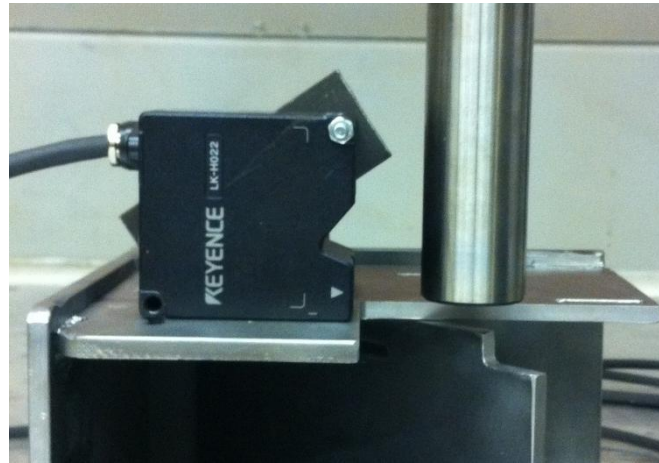


**Figure 3.10 – Dynamic resolution test setup**

Figure 3.11 shows the displacement data of the sensor when logging at 392 kHz with no averaging. As can be seen from the plot, when logging during a dynamic measurement, the noise on the signal increases significantly. This gives the appearance of the dynamic resolution to be approximately 10  $\mu\text{m}$ .

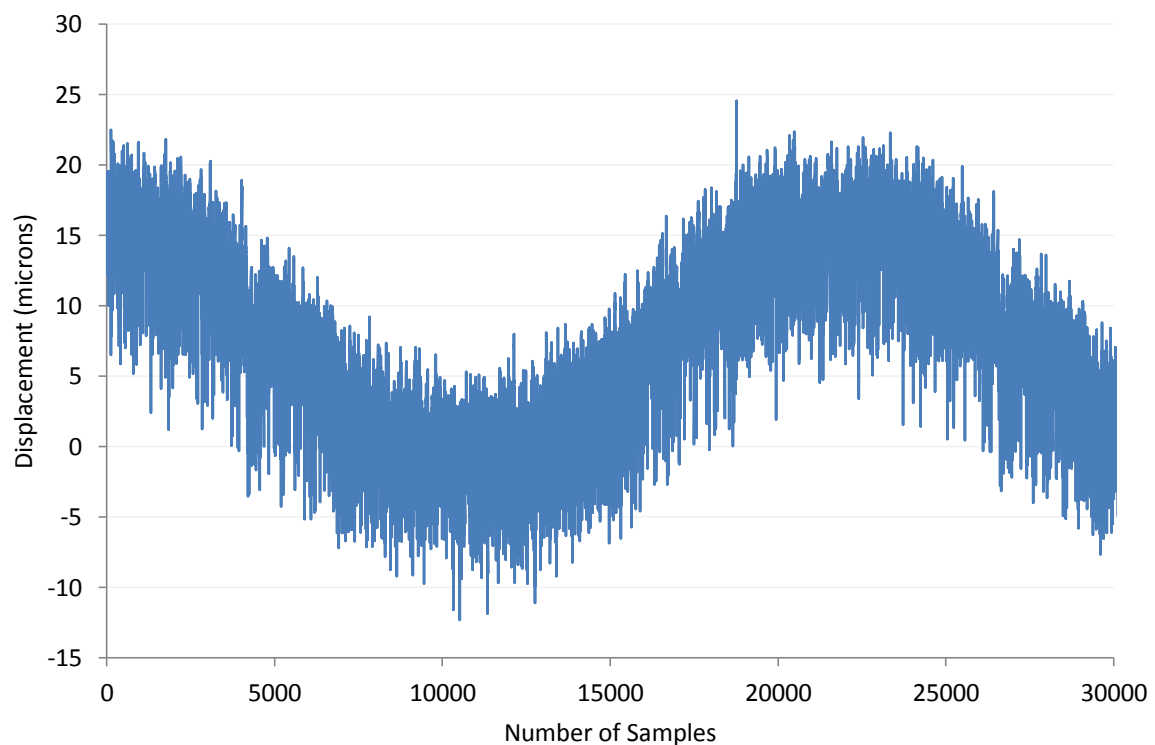


**Figure 3.11 – Dynamic resolution with 0 x averaging displacement data**

Using standard deviation on the data set to identify the potential dynamic resolution achievable with the sensor, gives 6.63  $\mu\text{m}$ . This is far outside the required resolution of 0.05  $\mu\text{m}$ .

### **3.2.5. Conclusions of Laser Testing**

The initial concerns about the sensors self heating were dispelled following good results from the warm up and thermal stability tests. Once the sensor had been allowed to warm up for 5 minutes the displacement output then remained stable to within 0.6  $\mu\text{m}$  for the two hour test duration. There still remained a slight concern about the affects the sensor would have on an ETVE test by adding to any externally induced heat.

The laser performed well under static resolution testing providing a possible resolution of 0.06  $\mu\text{m}$  when the data was averaged at 16 times (15 kHz sampling rate). However, when the laser was tested under dynamic conditions the resolution increased significantly to 6.63  $\mu\text{m}$  at 0 averaging. While this data could be averaged 16 times to bring it to a sample rate of 15 kHz, it would still be far outside the required resolution of 0.1  $\mu\text{m}$ .

This significant increase in noise was due to light scatter of the laser while trying to measure on a rotating surface. Keyence recommend setting the averaging to 16384 to stabilise the sensor reading, bringing the sampling rate down to 24 Hz. This is considerably lower than our required sampling frequency.

Therefore, while this sensor seemed to offer everything required on its specification, testing revealed that it was not suitable for the application of dynamic spindle analysis.



### 3.3. Eddy Current Testing

A number of eddy current sensors were investigated, a summary of which are listed in table 3, to find the most appropriate solution. Two sets of sensors were tested with the sensor that performed best during testing being described in this section. The results of testing from the other sensor can be found in the appendix.

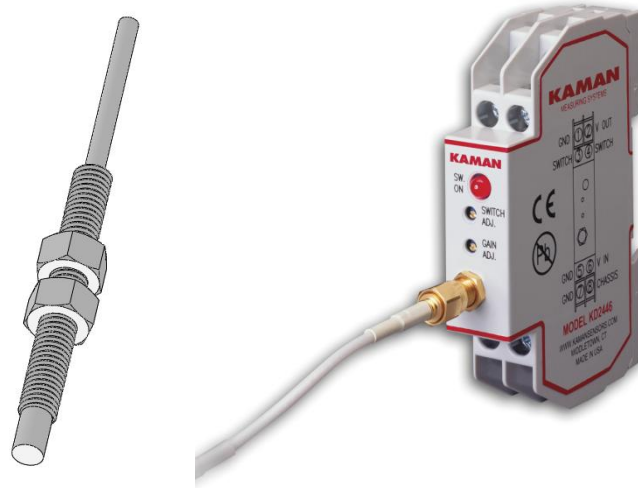


Figure 3.12 – Kaman eddy current sensor and signal conditioning unit

Figure 3.12 shows a CAD model of the Kaman eddy current sensor and the signal conditioning unit. When initial testing was conducted there were some concerns about the robustness of the system. When pressure was applied to the signal conditioning unit or it was moved during measurement, the sensor readout was affected. However, this was overcome by enclosing the signal conditioning units in a small robust case that ensured stability of the output (see figure 3.13).

#### 3.3.1. Thermal Stability

The aim of this test was to assess the thermal stability of the Kaman eddy current sensors and their signal amplifiers, firstly at room temperature and then with external heat source.

Two sensors were setup measuring against a steel surface to measure the change in temperature with change in ambient temperature, to assess the thermal stability of the sensors (see figure 3.12). Two temperature sensors were also setup, one to measure the ambient temperature near the sensors and the other to measure the ambient temperature of the signal conditioning unit.

Logging was initially for 1 hour to measure the stability of the sensors. After 1 hour the ambient temperature around the amplifier was heated up to 42°C and then left to cool, to assess the effect this had on the sensor output. The ambient temperature around the sensors was then heated to approximately 32°C to assess the effect this had on the sensor output and was then again left to cool.

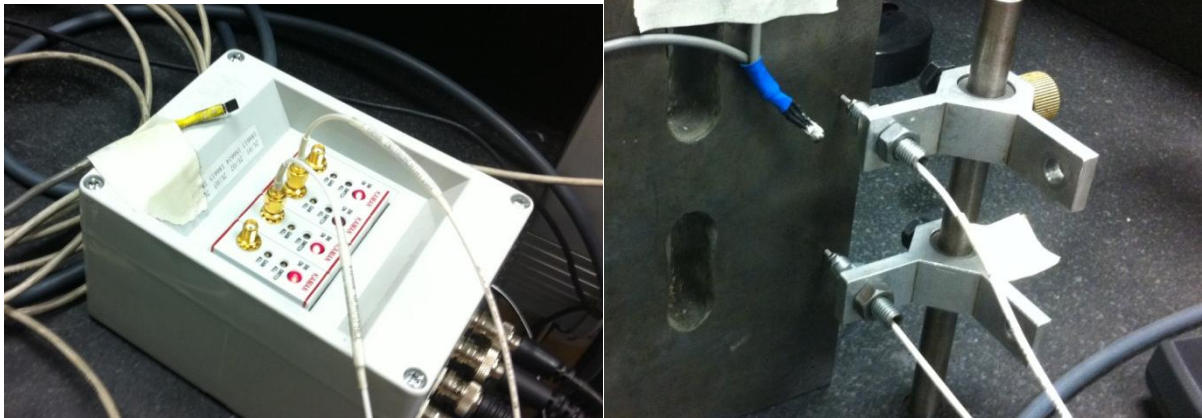


Figure 3.13 – Thermal stability test setup

Figure 3.14 below shows the temperature and displacement of the eddy current sensors and signal amplifier over the 100 minute test duration.

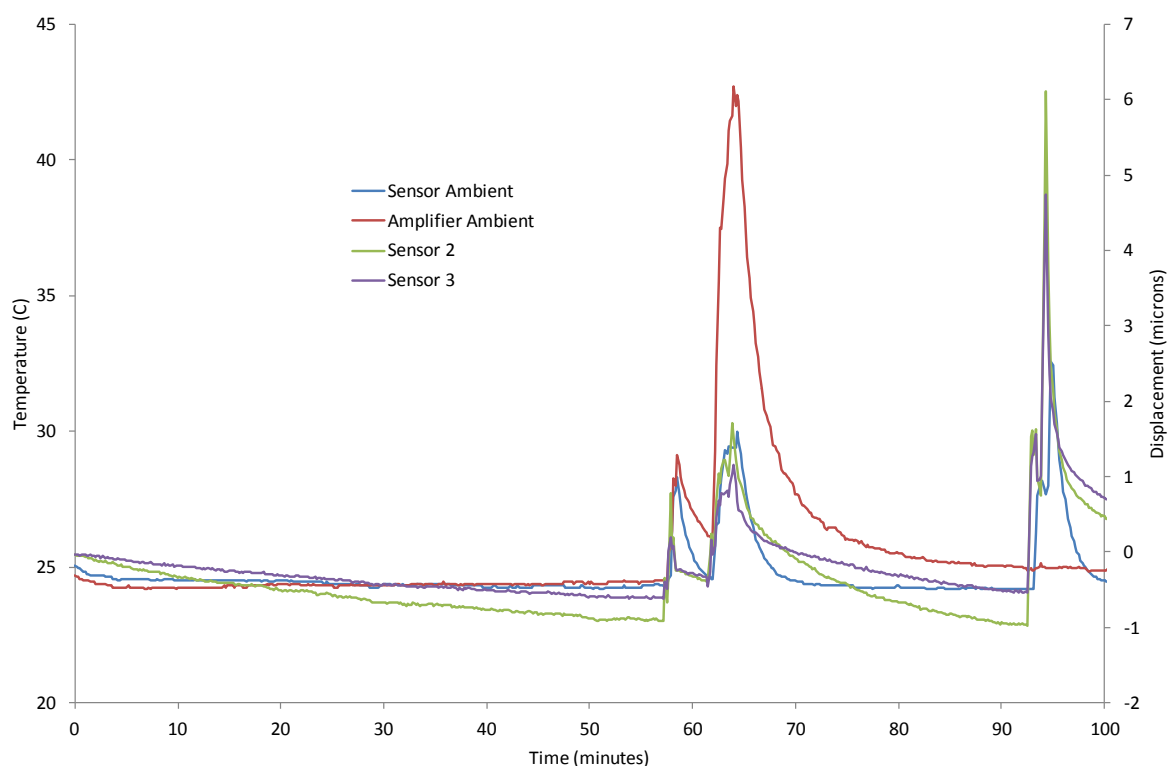
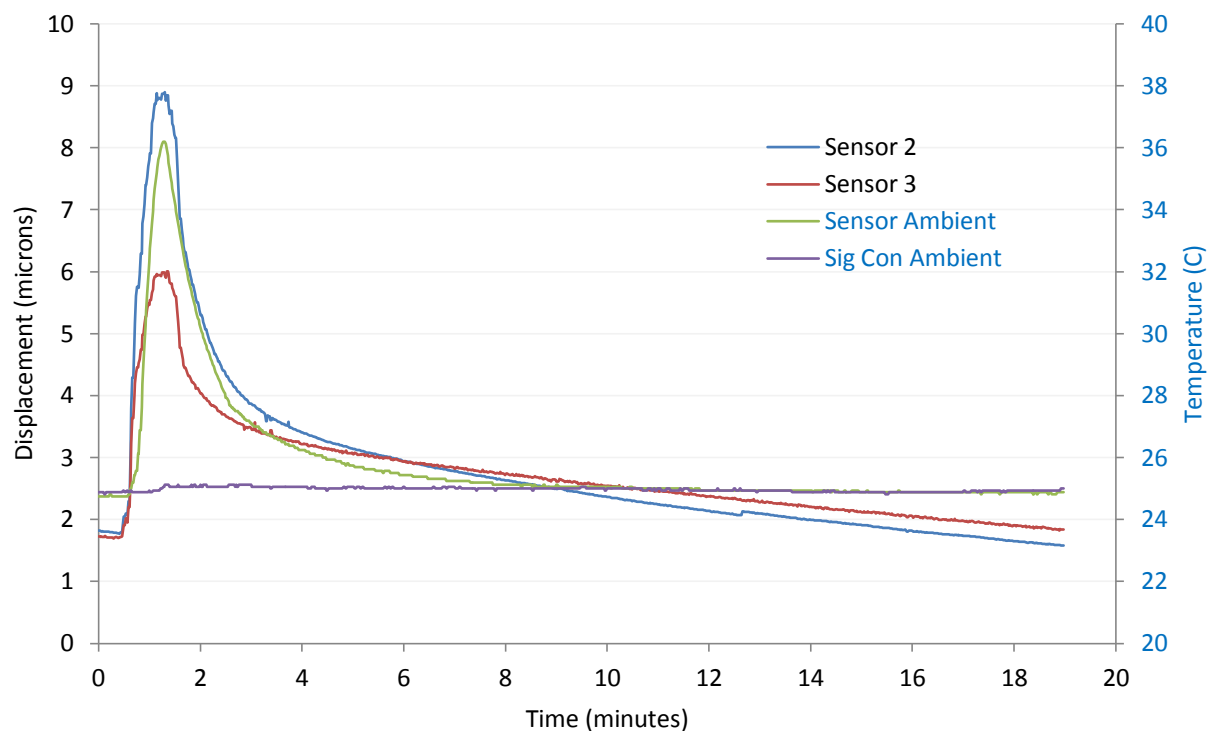


Figure 3.14 – Comparison of displacement and temperature during thermal stability test

During the first hour of the stability test the ambient temperature of both the sensors and the amplifier remained stable to within 0.5°C. This resulted in a displacement of sensor 2 and sensor 3 of 0.9  $\mu\text{m}$  and 0.6  $\mu\text{m}$  respectively.

The amplifier was then heated to 42°C which also heated the ambient of the sensors to 29°C, which resulted in a change in displacement of approximately 2  $\mu\text{m}$  in both sensors.

A second test was then performed by heating the ambient temperature around the sensor to 36°C logging the temperature and displacement every 2 seconds, as can be seen in figure 3.15.



**Figure 3.15 – Comparison of displacement and temperature during second thermal stability test**

The above plot shows a displacement of sensors 2 and 3 of 9  $\mu\text{m}$  and 6 $\mu\text{m}$  respectively. There is also a good correlation between the ambient temperature around the sensors and the displacement data.

Figure 3.16 shows the temperature plotted against the displacement of sensor 2 as the setup cools.

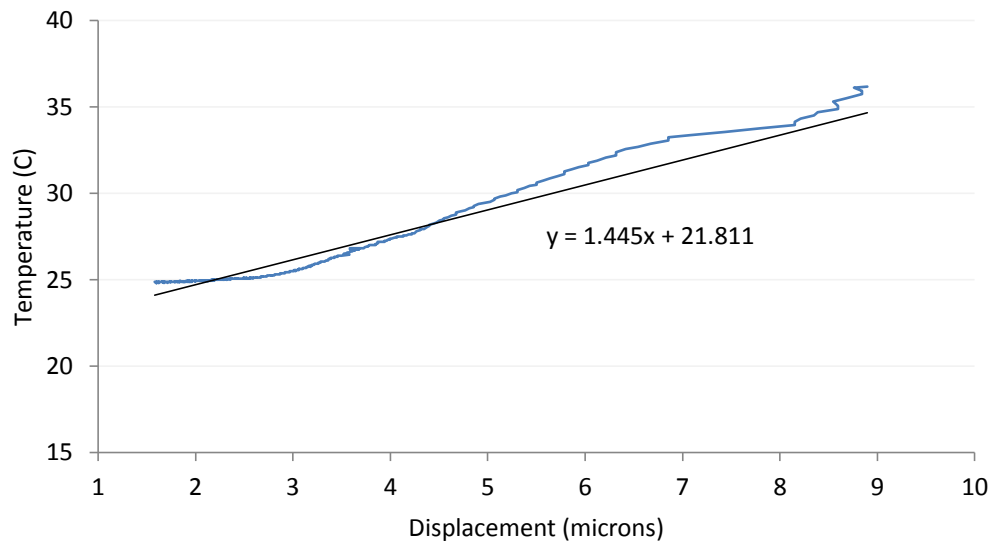


**Figure 3.16 – Sensor 2 temperature against displacement**

As can be seen there is a good linear relationship between the temperature and displacement indicating good thermal stability of the sensor. There is a change of  $0.69\mu\text{m} / ^\circ\text{C}$ .

Figure 3.17 shows the temperature plotted against the displacement of sensor 3 as the setup cools.

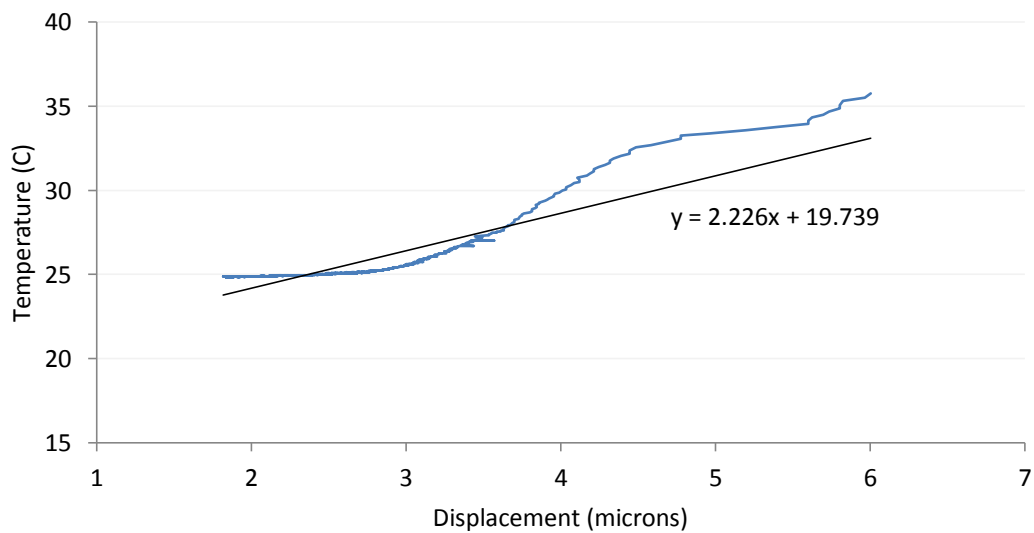


**Figure 3.17 – Sensor 3 temperature against displacement**

Again, there is a good linear relationship between the temperature and displacement indicating good thermal stability of the sensor. There is a change of  $1.08\mu\text{m} / ^\circ\text{C}$ .

The sensors were then left logging for a 50 hour period. Figure 3.18 shows the temperature and displacement data.

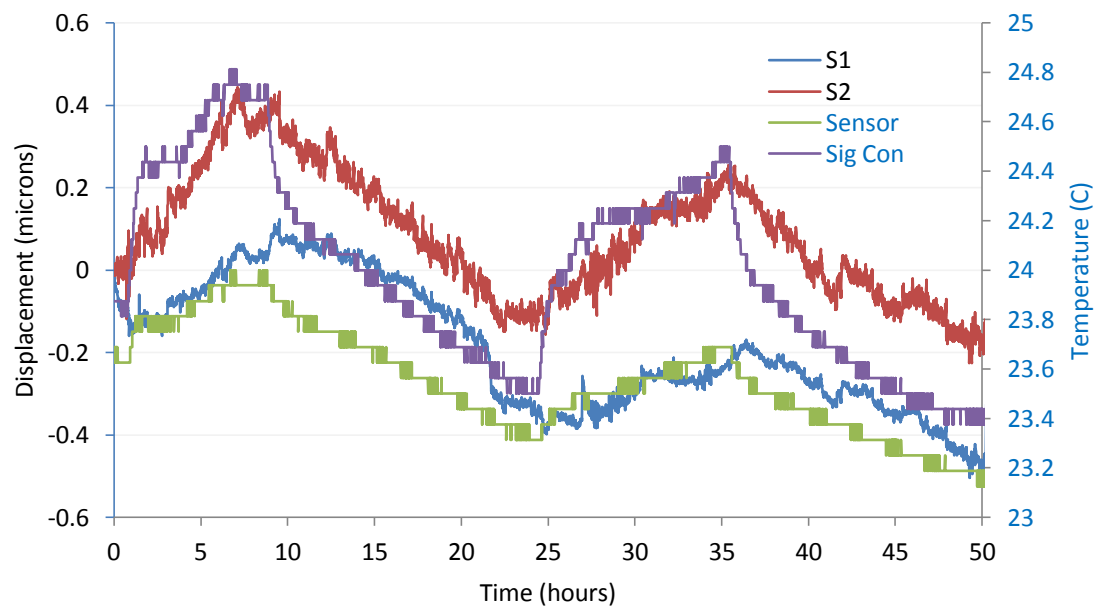


Figure 3.18 – 50 hour thermal stability test

The sensors displaced by approximately  $\pm 0.3 \mu\text{m}$ , showing very good thermal stability. There is also an excellent correlation between the ambient temperature data and the displacement.

### 3.3.2. Linearity and Calibration

The measurement range of the eddy current sensor is 500 $\mu\text{m}$ . However, only the first 100 $\mu\text{m}$  was required for the purpose of testing. This was due to the most sensitive section of the sensor appearing in this part of the range. The blue trace in figure 3.19 shows the output over the first 100 $\mu\text{m}$  and as can be seen the output is very non-linear.

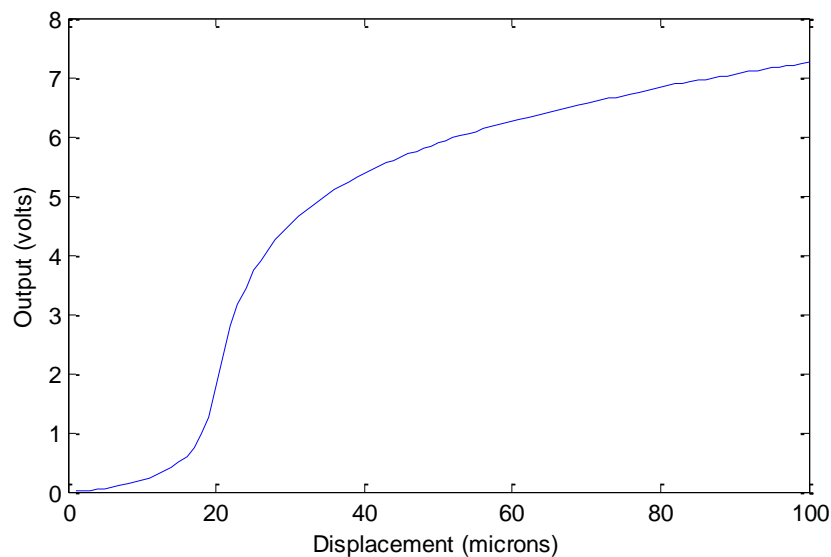
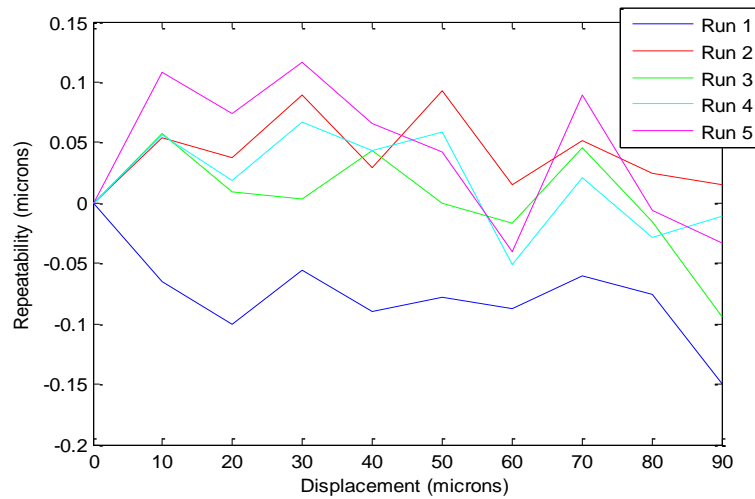


Figure 3.19 – Non-linear output from eddy current sensor

The output data file from this test was then input into Matlab and a curve fitting tool used to fit to the data. A low order polynomial was used to ensure robustness of the fit and to enable the fit to be performed to within 0.1 $\mu\text{m}$  the curve was chopped into sections. The end result is a calibration file for each individual part of the curve fit to within 0.1 $\mu\text{m}$  accuracy.

The data in figure 3.19 was captured using a 16-bit National Instruments (NI) data acquisition device and a bespoke computer application which uses standard NI APIs. The low order polynomial calibration file can then be loaded into the software whenever the sensor is being utilised with the target material for which it has been calibrated.

With the calibration file input into the windows application the repeatability of the calibrated sensor can be tested. The axis was moved in steps of 10  $\mu\text{m}$  in the same direction from the same starting position for five separate runs and the deviation from linearity plotted in figure 3.20.



**Figure 3.20 – Repeatability results for eddy current sensor output**

As can be seen the sensor measured repeatably to within 0.2  $\mu\text{m}$  over the 100 $\mu\text{m}$  range, validating the method.

### 3.3.3. Sensor Sensitivity Test

The sensitivity of the sensor was calculated and plotted over the first 40  $\mu\text{m}$  of the range, as this was the area where the non-linear section occurred. Figure 3.21 shows the peak sensitivity occurring at approximately 15  $\mu\text{m}$  from the beginning of the range.

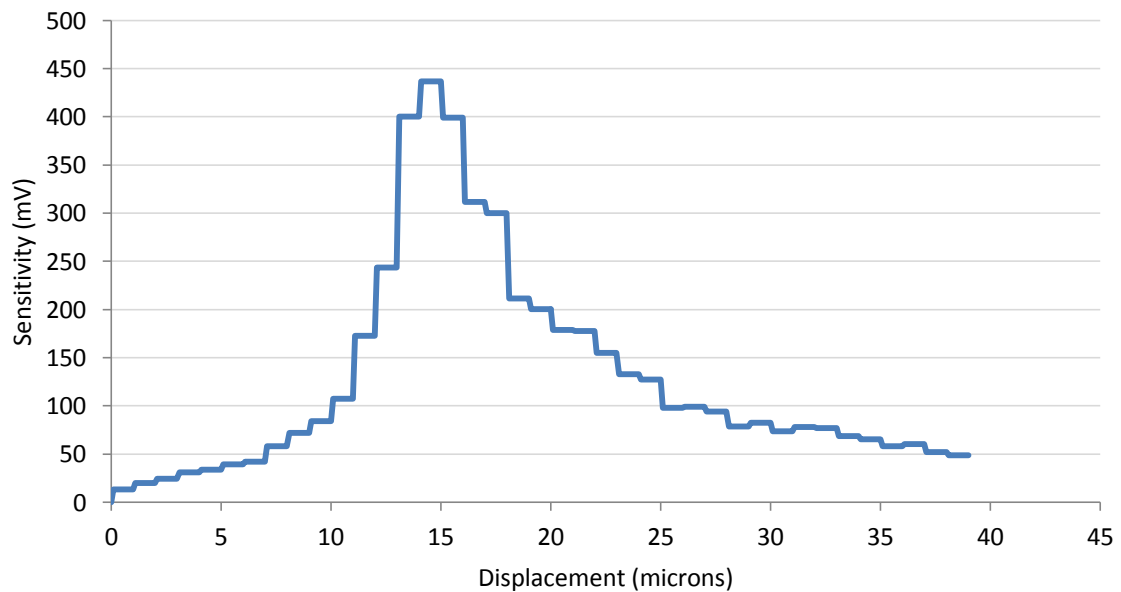


**Figure 3.21 – Repeatability results for eddy current sensor output**

### 3.3.4. Static Resolution Test

The aim of this test was to assess the static resolution of the sensor when measuring in the most sensitive part of the measurement range.

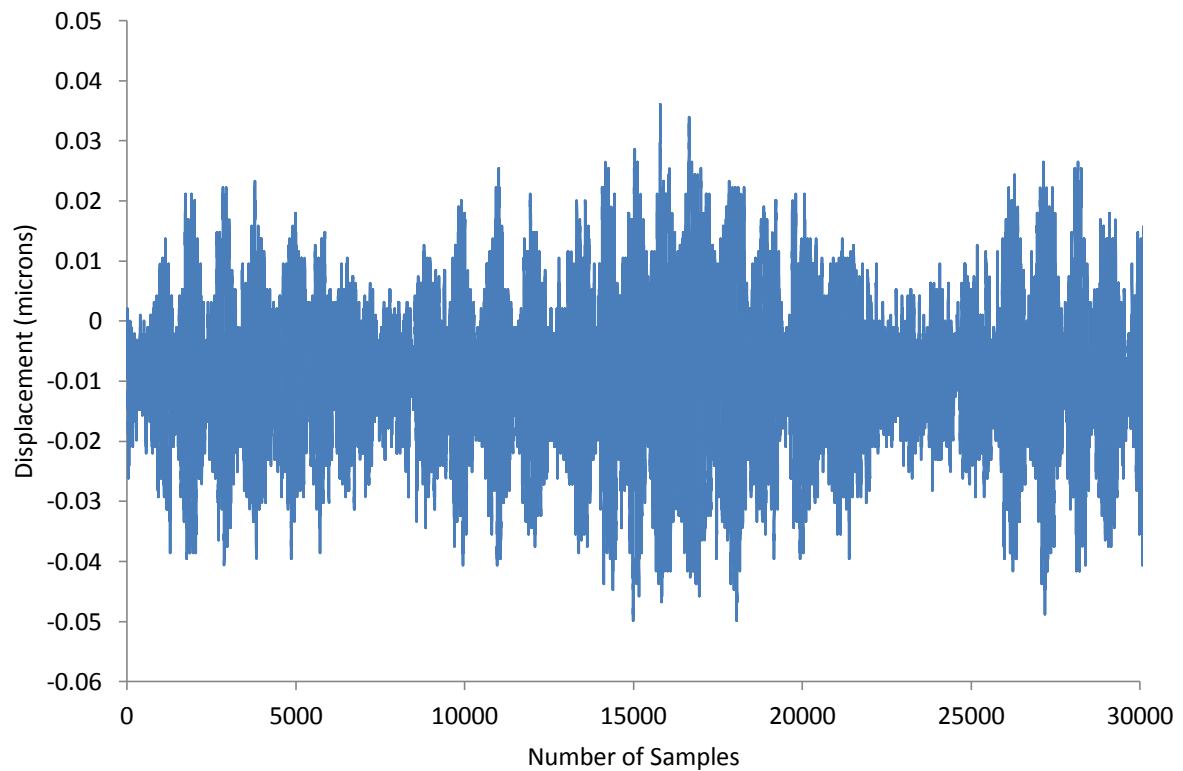
The test was carried out by positioning the sensor to measure off the same aluminium target as used during its calibration. The sensor was moved to the most sensitive part of the range determine the sensors highest static resolution. Data was logged at 10 kHz using a 16 bit National Instruments (NI) data acquisition device.



Figure 3.22 – Eddy current static resolution test setup

Figure 3.23 shows the displacement data of the sensor over 3 seconds when logging at 10 kHz. As can be seen from the plot, when logging during a static measurement, the displacement is approximately  $0.06\text{ }\mu\text{m}$ , which is comparable with the required resolution of  $0.05\text{ }\mu\text{m}$ .





**Figure 3.23 – Eddy current static resolution**

Using standard deviation on the data set to identify the potential static resolution achievable with the sensor, gives  $0.011\ \mu\text{m}$ , which is much better than the required resolution.

### **3.3.5. Dynamic Resolution Test**

The aim of this test was to assess the dynamic resolution of the sensor when measuring in the most sensitive part of the measurement range.

Using the calibration file that was previously created, a dynamic measurement was taken using a high resolution piezo actuated platform flexure rig. The eddy current sensor was set up to measure against the same target and the software loaded with the calibration file captured on a standard milling machine using the proposed method. A Renishaw XL80 laser interferometer was used as a traceable reference device (see figure 3.24).

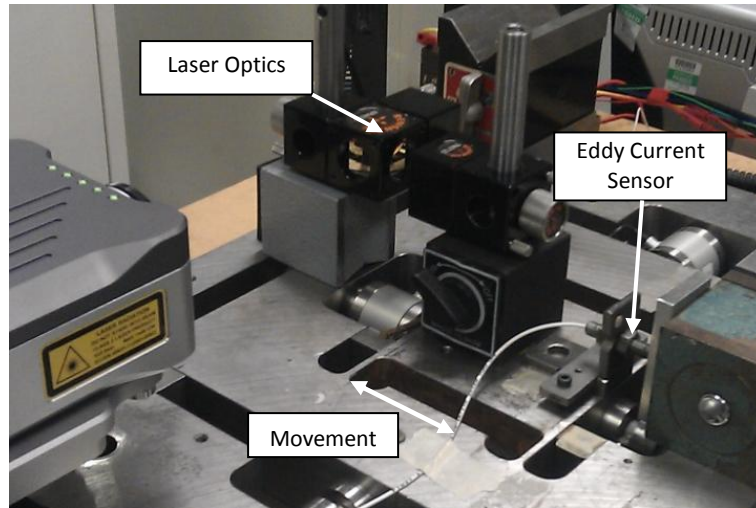


**Figure 3.24 – High resolution piezo platform dynamic resolution test setup**

The rig was set to vibrate at 100Hz and the magnitude of the oscillation adjusted to be approximately 0.008  $\mu\text{m}$  (this was the minimum magnitude before the signal became distorted). Figure 3.25 shows the output from the Renishaw XL80 laser interferometer. There are some imperfections of the sine wave but this is to be expected at this level of resolution and can be attributed to the stability of the setup.

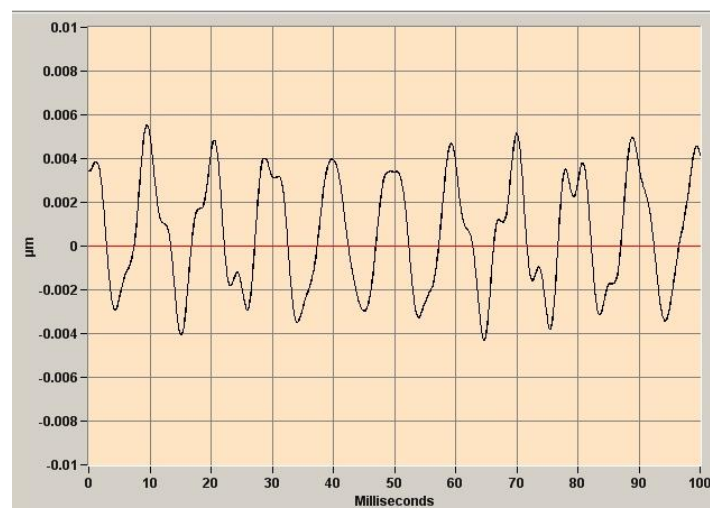


**Figure 3.25 – Renishaw XL80 laser output on vibration rig**

Figure 3.26 shows the output from the eddy current sensor sampling at 10 kHz. As is expected at this resolution there is some noise on the output signal but a sine wave can still clearly be seen at a magnitude of between 0.008 $\mu\text{m}$  and 0.01 $\mu\text{m}$ .

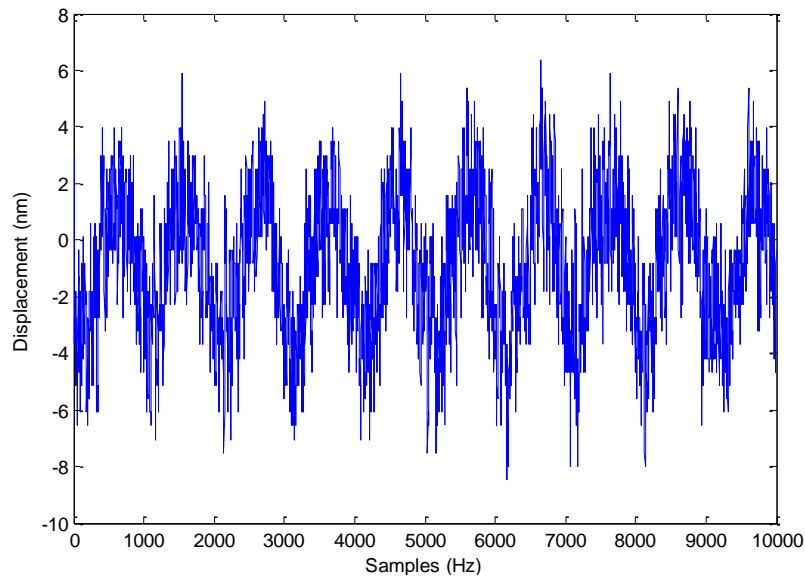


**Figure 3.26 – Output from eddy current sensor on vibration rig**

The standard deviation of the data in figure 3.26 shows the noise level to be at approximately  $0.0037\ \mu\text{m}$ . Since the data was sampled at 10 kHz averaging could be applied to clean up the signal, if this does not impinge on the required sampling frequency of the application.

### **3.3.6. Conclusions of Eddy Current Sensor Testing**

There were some initial concerns about the stability of the output signal due to the quality of the signal amplifiers. However, once these had been mounted in a rigid container the signal seemed a lot more stable and they performed extremely well during the thermal stability testing.

Due to the non-linearity of the sensors they required careful calibration to the intended target material. However, a method was successfully identified and implemented.

Static and dynamic resolution tests also showed the sensor to exceed the specifications with a very small  $0.008\ \mu\text{m}$  sinusoidal signal, correctly measured by the sensor. This indicates a theoretical sensitivity based on the standard deviation of less than  $0.004\ \mu\text{m}$  (4nm), which far surpasses the resolution requirement and would allow for testing of extremely high precision spindles.

The testing described in this section was on low cost un-calibrated eddy current sensors but by exploiting the non-linear output to get high resolution and calibrated to get accuracy, their suitability has been confirmed. Testing was also conducted on other eddy current sensors, which offer good linearity but the resolution is not quite as good, the results of this testing can be found in the appendix.

### **3.4. Capacitance Sensor Testing**

Testing was not carried out on any capacitance sensors as they have already been proven for use in spindle analysis. While this system offers a good solution, there are some limitations when it comes to practical spindle analysis.

Firstly, and most importantly, as previously mentioned the output of a capacitance sensor is affected by any particles present in the area between the sensor and the target. As a result, they may not be suitable for use in typical manufacturing environments, where swarf, dust and coolant may be present in testing areas and where the uncertainty of such effects cannot be eliminated through cleaning, because of the nature of application, a quick check by maintenance departments or even by operators.

The system only utilises 5 channels, for measuring error in X, Y and Z and a further two sensors measuring in X and Y for tilt. It is sometimes beneficial to use a 6<sup>th</sup> channel during thermal testing to offer a differential between the spindle nose and the end of the test-bar.

The commercial systems available at the time of writing this report are very expensive and therefore may not be a viable option for the majority of small to medium size enterprises (SME's) looking to implement spindle analysis processes. Tables 3 and 4 examine typical costs per channel.

### **3.5. Non-Contact Sensor Solution**

There are many factors to consider when choosing the most suitable non-contact sensor, the most important of which were identified at the beginning of this section. The testing described has assessed the prospective sensing technologies against these criteria to establish their suitability.

Testing and research was carried out on further sensors not mentioned in this section. Results from this testing can be found in the appendix, with the rest of the information gathered taken from the manufacturer specifications.

The following pages display all investigated non-contact sensors in table form to allow for comparison.

Table 3 – Comparison of Non-Contact Measurement Sensors Part 1

SENSOR TYPE	EDDY CURRENT (OLD MICRO EPSILON)	LION PRECISION SYSTEM	RIFTEK LASER	SMALL EDDY CURRENT (4U ON KD-2446)	SMALL EDDY CURRENT (2U ON KD-2446)
Spot Size	22mm <sup>2</sup>	-	≈ Φ 30 μm	11.3mm <sup>2</sup>	3.14mm <sup>2</sup>
Range	1mm	250μm	2mm	1.3mm	0.5mm
Offset	≈0.2mm	125 μm	10mm	≈0.2mm	≈0.2mm
Max Sampling Frequency	9kHz	15kHz	8kHz	10kHz	10kHz
Resolution	≈0.1μm	15nm	0.6 μm	0.1 μm	0.04 μm, Varies
Output Voltage Range	0 – 10 VDC	±10V	0 – 10 VDC	0 – 10 VDC	0 – 10 VDC
Cost / channel	Circa £2,000	N/A	£785.00	£785.00	£610.00
Temperature Range	-	4°C – 50°C	-10°C – 60°C	-10°C – 60°C	-55°C - 105°C
Environmental Resistant	YES	NO	NO	YES	YES
Sensitivity of input Voltage	N/A	N/A	Negligible	None (12-24v)	None (12-24v)

## NOTES

Values in red are taken from manufacturer specifications  
Values in blue are results of testing conducted on the sensors

Table 4 - Comparison of Non-Contact Measurement Sensors Part 2

SENSOR TYPE	MICRO EPSILON LASERS	KEYENCE LASERS (LK-G-32)	KEYENCE LASERS (LK-H022)	CAPACITEC CAPACITANCE SENSORS	LION CPL 190 DRIVER SYSTEM
Spot Size	≈ Φ 30 μm	Φ 30 μm	Φ 25 μm	-	-
Range	2 mm	10 mm	6 mm	2 mm	500 μm
Offset	10 mm	30 mm	20 mm	0.5 mm	250 μm
Max Sampling Frequency	10 kHz	50 kHz	392 kHz	15 kHz	15 kHz
Resolution	0.03 μm	0.05 μm	0.02 μm, varies	TBC	10nm
Output Voltage Range	-	-	-	0 – 10 VDC	±10V
Cost / channel	TBC (≈ £4k)	£2423.00	£3486.97	£2884.28	£4047.00
Temperature Range	-	0°C – 50°C	0°C – 50°C	-	-
Environmental Resistant	No	No	No	No	No
Sensitivity of input Voltage	-	-	-	-	-

## NOTES

Values in red are taken from manufacturer specifications  
Values in blue are results of testing conducted on the sensors

Through experimentation it has been found that in some cases the manufacturer's specifications is not always what is achievable in the required applications.

Table 5 details the advantages and disadvantages of all 3 of the best performing potential non-contact sensing technologies.

**Table 5 – Advantages and Disadvantages of the Potential Systems**

SYSTEM	ADVANTAGES	DISADVANTAGES
PROVEN CAPACITANCE SYSTEM	<ul style="list-style-type: none"> <li>• It is a proven system</li> <li>• It has full traceability of measurement</li> <li>• Excellent resolution</li> <li>• Can be used on any target material</li> <li>• Can be used on small targets</li> </ul>	<ul style="list-style-type: none"> <li>• Very Expensive. May be exacerbated by requiring dual range system or multiple systems to measure error motion and thermal on a range of spindles</li> <li>• Long lead time on kit and possible spares</li> <li>• Limited to a 5 channel system</li> <li>• Low maximum sampling frequency compared to laser systems</li> <li>• Must be used in clean environment</li> <li>• Very small target range</li> </ul>
KAMAN EDDY CURRENT	<ul style="list-style-type: none"> <li>• Very inexpensive</li> <li>• Can be used in dirty manufacturing environments</li> <li>• High sensitivity over short range enables high resolution to be achieved</li> <li>• Good measurement range to resolution ratio</li> </ul>	<ul style="list-style-type: none"> <li>• Sensors need calibrating to the target material</li> <li>• Require a larger target area, although the miniature sensor head is just 2mm in diameter, requiring only a 6mm target</li> </ul>
KEYENCE LASER LK-H022	<ul style="list-style-type: none"> <li>• Extremely high sampling frequency, allowing for high speed testing without reduced accuracy</li> <li>• Large offset and range for ease of setup and reduced risk of damage</li> <li>• Very small spot size, so extremely small targets can be used allowing for higher rpm testing</li> </ul>	<ul style="list-style-type: none"> <li>• Relatively expensive</li> <li>• Resolution during dynamic measurement is very poor due to light scatter</li> <li>• Sensors are large, making fixture design difficult</li> <li>• Sensor heads get very warm so fixtures need to be thermally stable</li> </ul>



After comprehensive testing and careful consideration of the key elements and requirements of the type of sensor to be utilised, the Kaman eddy current sensor was chosen as the most suitable for the required application.

This sensor fulfilled all the key requirements of resolution, sampling frequency and range, whilst also offering the added benefit of being able to be used in manufacturing environments. They are also very inexpensive in comparison to the other sensor options, enabling a more affordable overall system to be produced, which must be considered as a key motivating factor for broader application of this important measurement.

## **4.0 System Design**

---

The selection of an appropriate displacement sensor completes one of the main parts of the project. To enable spindle analysis testing to be carried out to ISO standards, further system hardware and software needed to be designed and manufactured.

### **4.1. Equipment Design**

The main elements of hardware to be identified or design are:

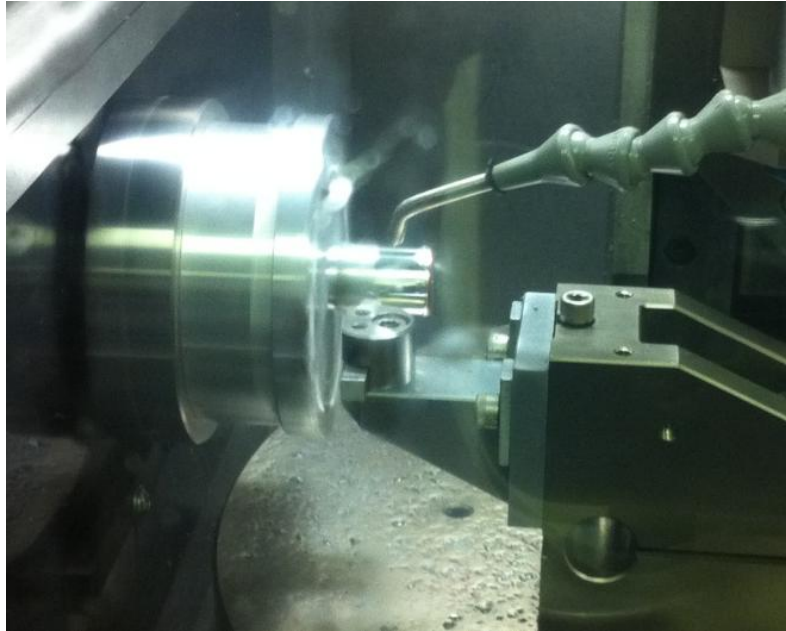
- Precision Test-bars
- Fixtures
- Data Acquisition Device

The design of suitable test-bars and fixtures is very important to enable high accuracy measurement to take place.

#### **4.1.1. Test-bar Design**

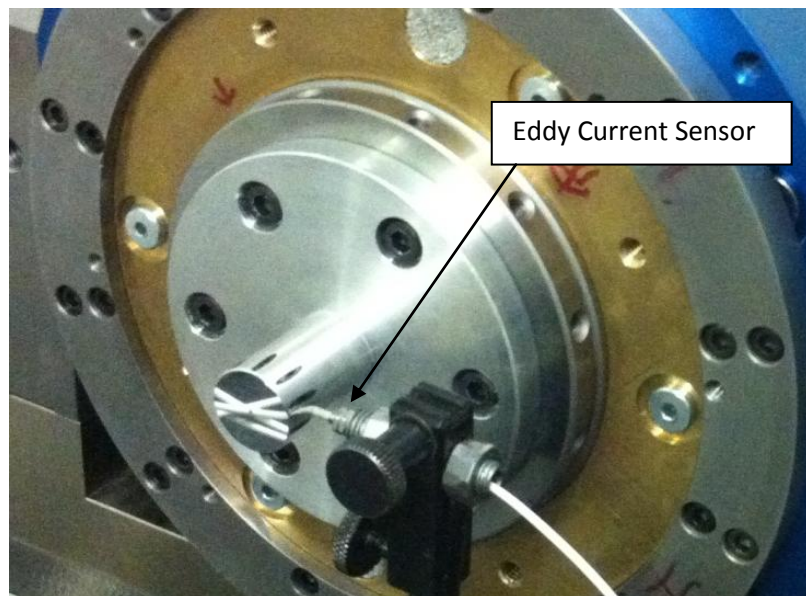
Although electrical run-out (see section 2.2.4) can be removed using one of the reversal methods, it is a good idea to limit it so that it does not dominate the signal. Aluminium has one of the lowest permeability values available, so for error motion measurement, aluminium test-bars were developed.

Figure 4.1 shows the manufacture of a short test-bar on a diamond turning machine with a radial and axial run-out of <50nm. The test-bar was initially machined on a standard turning machine and a target area (20mm in length) machined at a very low material removal rate with a diamond tipped cutter to produce a high precision mirror finished target area.



**Figure 4.1 – Manufacture of short aluminium test-bar**

Figure 4.2 shows the short aluminium test bar being used on a high precision air bearing spindle measuring the radial error motion.



**Figure 4.2 – Short Test-bar measuring radial error motion**

Figure 4.3 shows a long aluminium test-bar being used to measure the tilt error motion of a spindle. This was manufactured using the same method as the short test-bar, only this one required two precision surfaces at a set distance of 100mm, apart to facilitate the measurement of tilt.



**Figure 4.3 – Long Test-bar measuring tilt error motion**

The test-bars have a diameter of 20mm, as the eddy current sensors selected are a 2mm diameter unshielded model. The unshielded eddy current sensors require a target area 3 times that of the sensor diameter, therefore a minimum target area of 6mm diameter is required. As two sensors are required to measure in two directions, it is important their magnetic fields do not interfere with each other. To ensure sufficient distance between sensors a 20mm test-bar was chosen.

When using the flanged test-bars in figures 4.2 and 4.3 on a spindle with a face plate interface, there is no fine adjustment for centring them. The adjustment comes from the clearance of the bolt holes and requires the test-bar to be tapped into position. Using this method it is difficult to achieve a test-bar run-out of less than  $1\mu\text{m}$ . It can also be extremely time consuming, especially as the setup needs to be done twice per error measurement.

When performing spindle analysis on a milling spindle with a tool holder interface, an un-flanged test-bar can be used with precision collets that typically provide a run-out of  $<3\mu\text{m}$ . This is an acceptable level of run-out for a ball bearing spindle, but when measuring a high precision air bearing spindle a run-out of  $<1\mu\text{m}$  is required to achieve the required level of resolution. This is due to the high sensitivity area of the sensor only being over a small range.

Manufacturing the test-bars out of aluminium means that they are not ideal for thermal testing due to its high expansion coefficient. The thermal expansion of the test-bar could be calculated and removed from the data, if the temperature of the test-bar could be monitored to a sufficient level of accuracy.

Alternatively, a test-bar manufactured from a thermally stable material such as Invar may be preferable.

#### **4.1.2. Fixture Design**

A set of fixtures has been developed for mounting the eddy current sensors during spindle analysis. The fixture allows for adjustment in two planes so that the sensors can be positioned within the required measuring range and the point where the sensitivity of the sensor is at its highest.

The fixture is manufactured from 10mm thick steel for structural stability. When measuring at a sub micron level, it is important to reduce the external influences of vibration as much as possible. By having a thick steel fixture it increases the stability of the setup and reduced the amount of vibration induced into the sensors, which may affect the measurement.

Figure 4.4 shows the adjustable fixture being used to measure the radial error motion in the X and Y directions.



**Figure 4.4 – Adjustable fixture of radial error motion testing**

When measuring thermal displacement, the steel fixtures are not appropriate, as the thermal expansion properties of steel would influence the accuracy of the measurement. Figure 4.5 shows the use of Invar bar and fixtures during a thermal test. Invar has a very low thermal coefficient of expansion and so is a perfect material for manufacturing the fixtures.

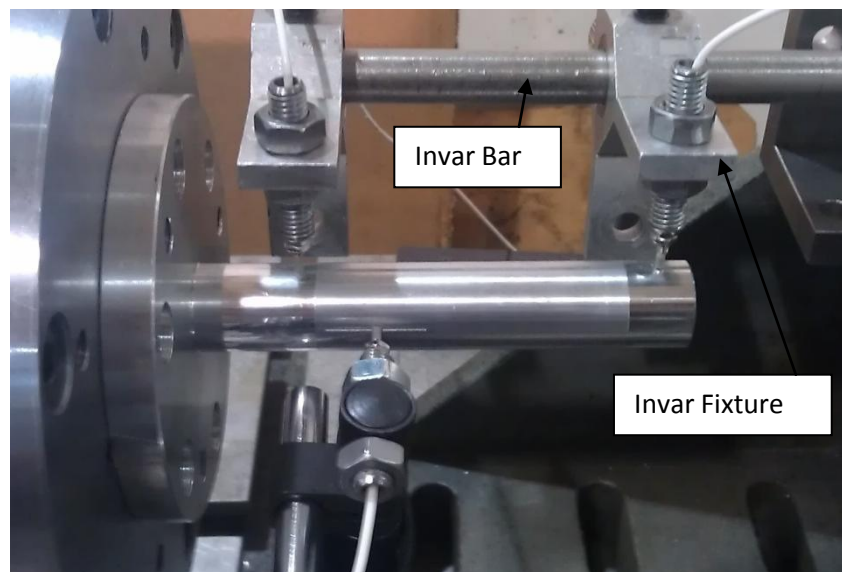


Figure 4.5 – Invar fixture for thermal testing

Further development of the fixtures would be beneficial, to allow for sub micron level adjustment, which would reduce setup times. A five sensor nest would allow simultaneous measurements to take place and enable thermal measurements to be taken using the same setup if manufactured from a thermally stable material such as Invar.

#### 4.1.3. Data Acquisition

A data acquisition device and logging software are also required, to capture and log the data from the sensors. The required device must have the following:

- 8 channels – to allow scope for additional sensors to be used if necessary
- 16-bit resolution – this allows potential measurement to a resolution of 1nm
- Capable of voltage logging
- Simultaneous sampling – to enable accurate measurement at faster speeds



**Figure 4.6 – National Instruments data acquisition device**

Figure 4.6 shows a suitable data acquisition device from National Instruments. For ease of use, this device has a USB connection to the laptop or PC to be used for data capture. It works with NI signal express software, which is a basic NI software, for which a low cost software licence can be obtained.

## 4.2. Data Processing

It is necessary to convert the raw voltage recorded by the NI software to microns, following data capture. This data will then require processing to put it into a usable format for data interpretation. The method of processing the data varies depending on the type of spindle testing; the following section describes how this is done for each type of spindle analysis test.

### 4.2.1. Thermal Data Processing

The amount of post processing required with thermal data depends on the type of test bar used. Previous methods of thermal testing implemented the use of a steel test-bar which had a large form error of approximately 20  $\mu\text{m}$ . If a test-bar such as this, with a large run-out, is used then the data needs to be averaged out so the magnitude of thermal growth can be determined. If a test-bar with a small run-out (in the order of 1 $\mu\text{m}$ ) is used then it may be possible to use the raw data without averaging, assuming that the thermal error is of sufficient magnitude.

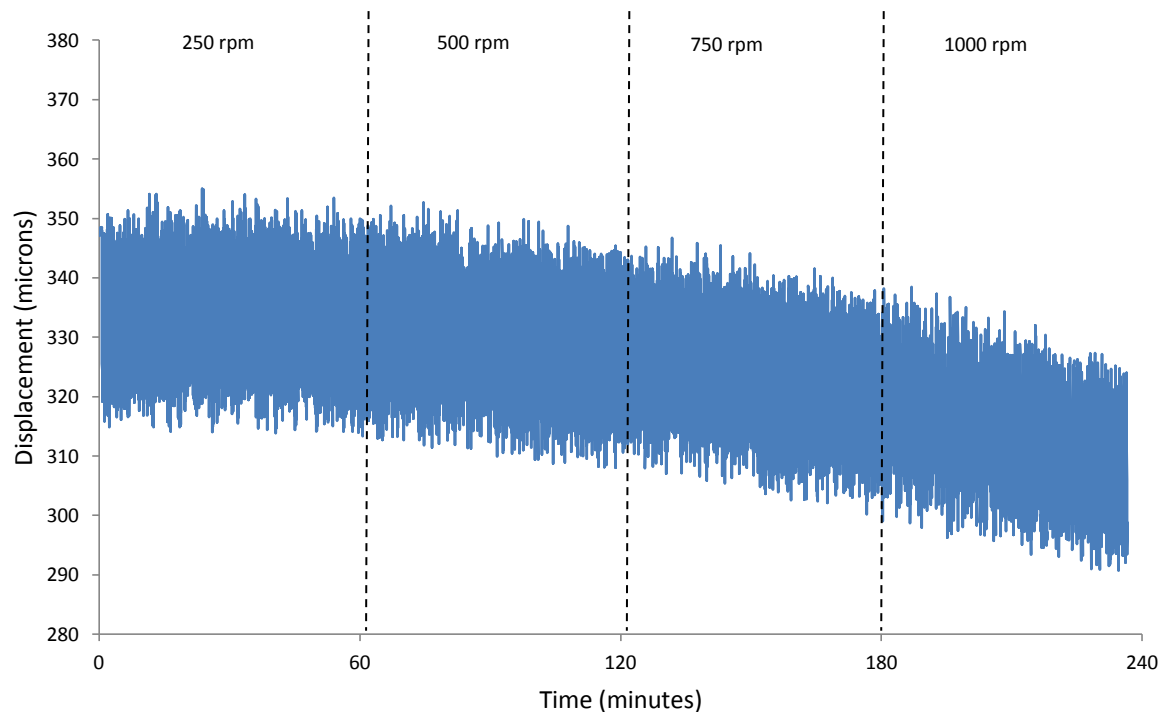
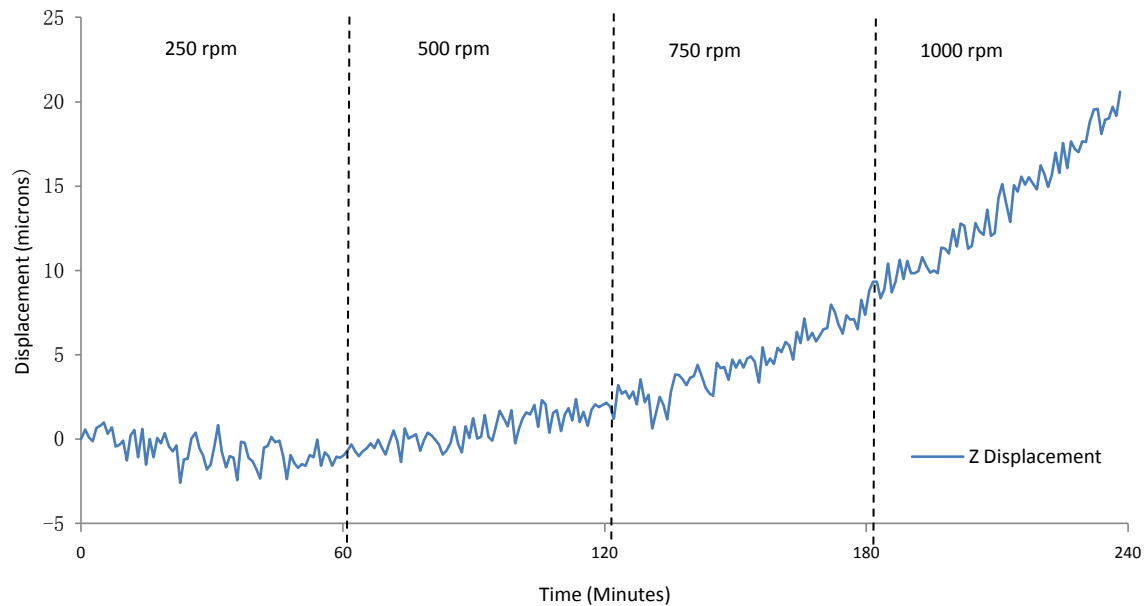


Figure 4.7 – Raw thermal data plot converted to microns

Figure 4.7 shows the Z-axis displacement of a spindle during a 4 hour step heating test, with the raw voltage data converted into microns. As can be seen, the test-bar run-out is approximately 30 $\mu\text{m}$  and it is only possible to obtain a rough order of magnitude of the spindle displacement. The data



was averaged and inverted to produce the plot in figure 4.8, which displays more clearly the displacement of the spindle in the Z-axis direction to be approximately 20 $\mu\text{m}$  over the 4 hour run time.



**Figure 4.8 – Post processing averaged data plot**

Thermal displacement data on its own is not that meaningful. It is important to monitor temperature at various points around the machine as well, so that the cause of thermal expansion can be identified. This can be done by using cheap surface mountable temperature sensors to measure areas of thermal interest, as seen in figure 4.9.

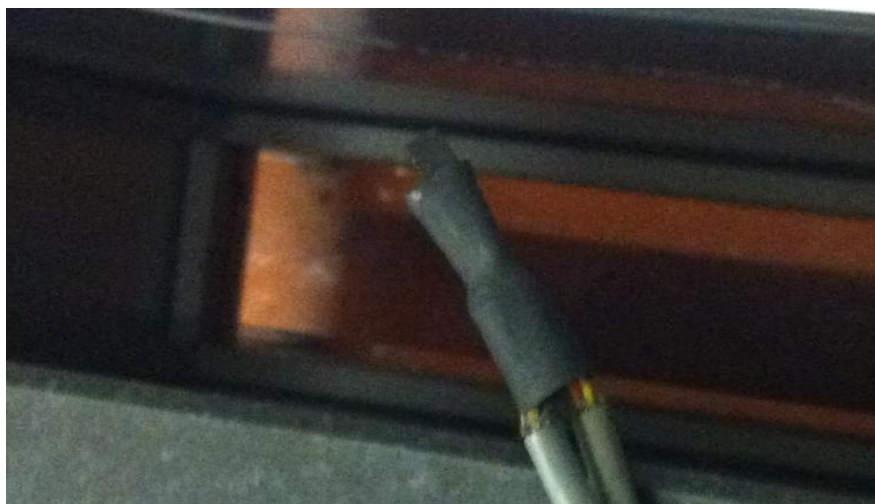


**Figure 4.9 – Surface mountable temperature sensor**

These sensors offer an accuracy of  $\pm 0.5^{\circ}\text{C}$  from  $-10^{\circ}\text{C}$  +  $85^{\circ}\text{C}$  with a unique 1-wire interface which requires only one port pin for communication. They can be easily assembled in series for positioning around a machine tool, with extension wires for use on larger machines. Each device has a unique 64 bit serial code in an onboard ROM so each sensor can be easily identified and labelled appropriately during data logging. The price per unit is approximately £2, so a full temperature measurement system can be assembled for a very affordable price.

Figure 4.10 shows the associated temperature data from the displacement data in figure 4.8. The temperature is logged from the temperature sensors using specialist software and plotted against time to show the change in temperature during the test period.

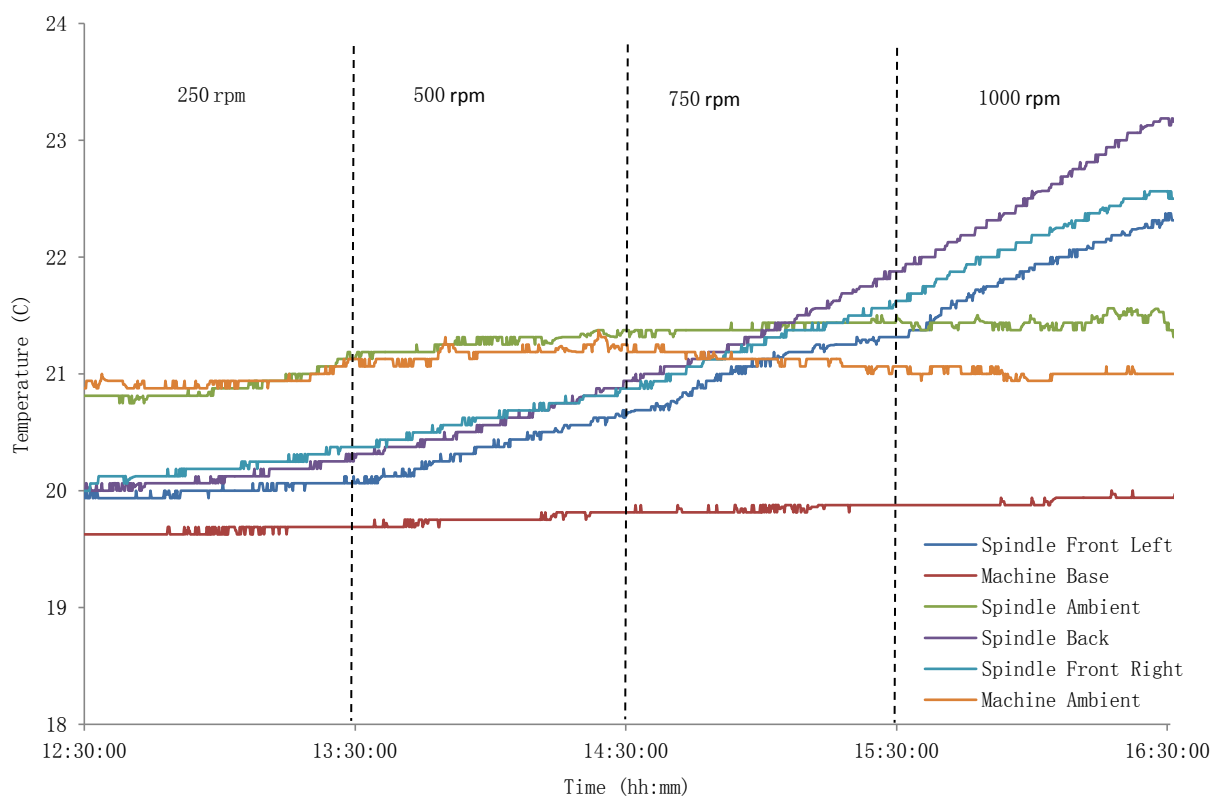


Figure 4.10 – Temperature data

#### 4.2.2. Geometric Data Processing

Data obtained from geometric testing requires the most amount of processing following capture. When measuring high accuracy spindles with radial run-outs in the order of  $1\mu\text{m}$  or less, then test-

bar run-out and form error cannot be ignored. Also, as mentioned in the literature review, when using eddy current sensors electrical run-out error is also present in the signal. All of these errors can be removed through the use of the following reversal technique.

#### 4.2.2.1. Donaldson reversal method

This method requires the fewest measurements (two), although setup time maybe increased. The method works by taking two measurements, one in the forward direction and one in the reverse direction. In the forward direction setup, the angular position of the spindle rotor, the spindle stator and the test-bar and the eddy current sensor are all aligned. In the reverse direction setup, the eddy current sensor and the test-bar are rotated through 180° with respect to the spindle rotor and spindle stator, as can be seen in figure 4.11.

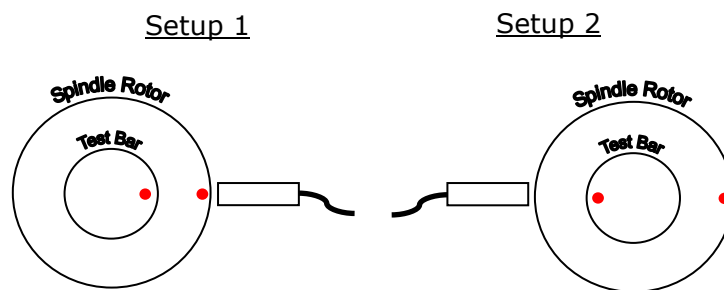


Figure 4.11 – Donaldson reversal technique [20]

The two measurements are a combination of the spindle's radial error motion and the test-bar run-out, test-bar form error and electrical run-out. Using the following mathematical equations, the two can be separated.

$$Testbar\ Error = \frac{Setup\ 1 + Setup\ 2}{2}$$

$$Spindle\ Error = \frac{Setup\ 1 - Setup\ 2}{2}$$

Other methods of are available for the removal of test bar form error and electrical run-out.

As mentioned in the literature review, Marsh [20] suggests using a slightly eccentric target to provide a once per revolution component to the output data. This can introduce unwanted vibration from an out of balance test-bar, when measuring at high precision levels of accuracy.

To overcome this, another method for measuring the angular position of the test-bar with respect to the spindle was devised that uses a small mark in the test bar and an additional sensor to detect the mark (this sensor is available because not all are used for dynamic measurement). This can then be correlated with the mark from the second set of data to ensure the two data sets match up, even if small variations in the rotational speed of the spindle occur. Figure 4.12 shows the run-out data from the sensor with a sharp peak where the mark on the test-bar is located. Using a combination of low pass filtering and a peak finding function in Matlab the individual peaks can be identified.

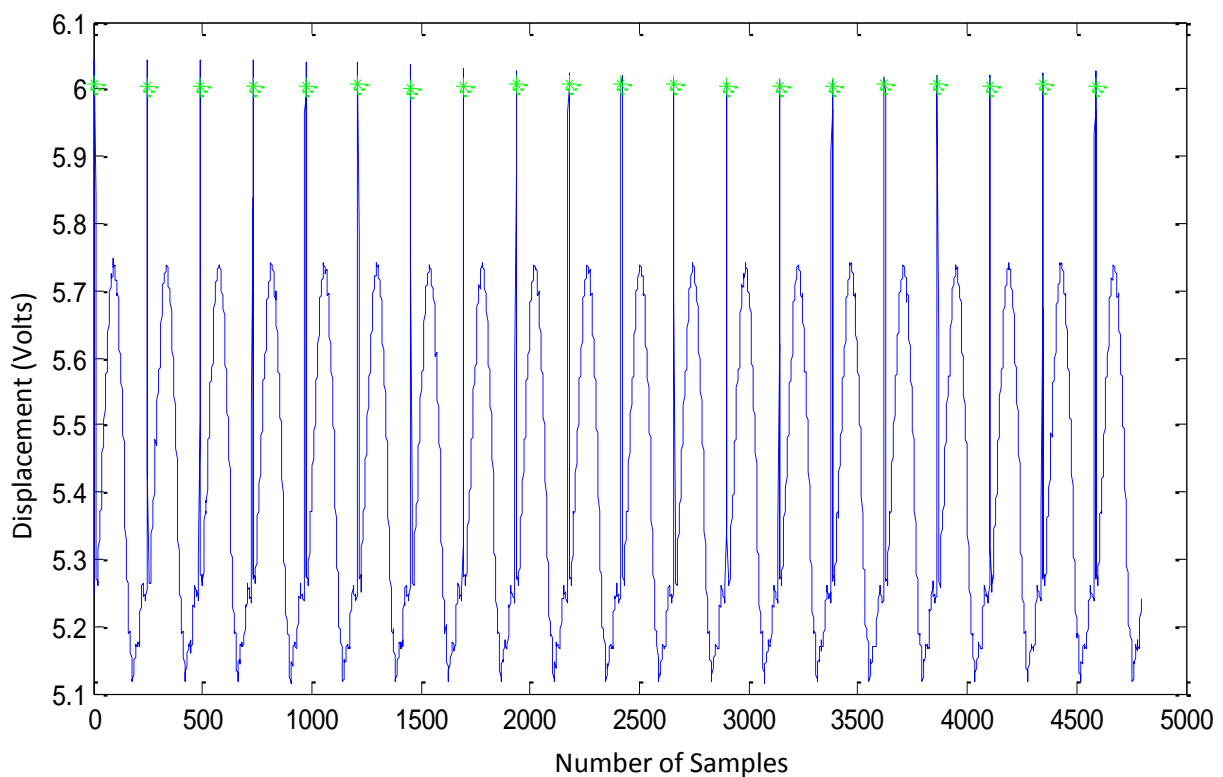


Figure 4.12 – Peak finding data

This is important when measuring spindles where the rotation speed may not be constant and therefore there will be a differing number of samples per revolution. By identifying the peaks the

number of samples per revolution can be found and the data interpolated to match up exactly with the data from the reverse direction setup.

Figure 4.13 shows a zoomed in peak, and as can be seen the profile of the mark is not a smooth curve. It is therefore important not to choose the highest peak as this could vary, but to use a low pass filter so that the once per revolution peak is more accurate. As can be seen from figure 4.13, the mark for the peak is central despite the rough extents of the mark.

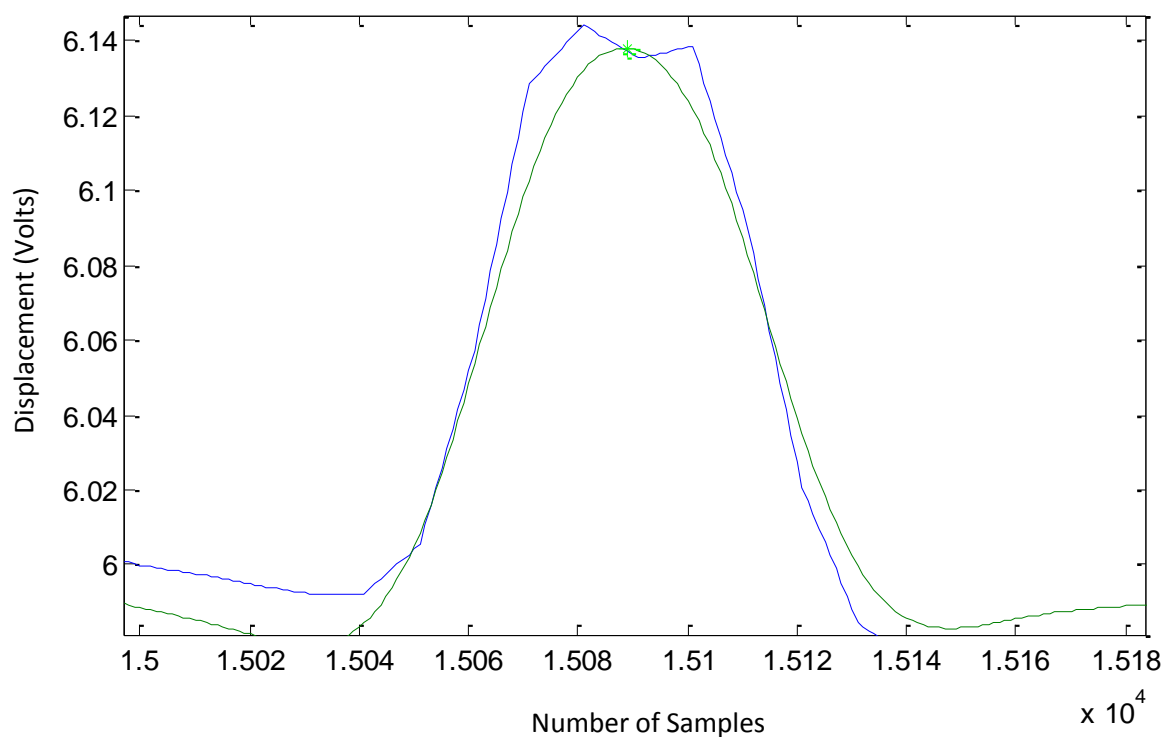


Figure 4.13 – Peak finding data

#### 4.2.3. Vibration Data Processing

Due to the high sensitivity of the sensors over a small range, it is possible to take vibration measurements to identify the magnitude of spindle vibration frequencies. This can be either a measurement taken on a static structural part of the spindle or a dynamic measurement taken against the test-bar.

The data is the same raw voltage output file from the eddy current sensors as used in the other test. This can be input into Matlab and used in a Fast Fourier Transfer (FFT) function to produce an FFT plot, which can identify resonant frequencies in the spindle. An example of this can be seen in figure

4.14, which shows data taken from a high precision air bearing spindle. As can be seen, the vibration is dominated by the rotation frequency of the spindle, as would be expected with a spindle of this quality. At 1000rpm the spindle rotation frequency is 16.67 Hz, which is the frequency of the first peak in the plot below; the repeated peaks are harmonics of the rotational speed.

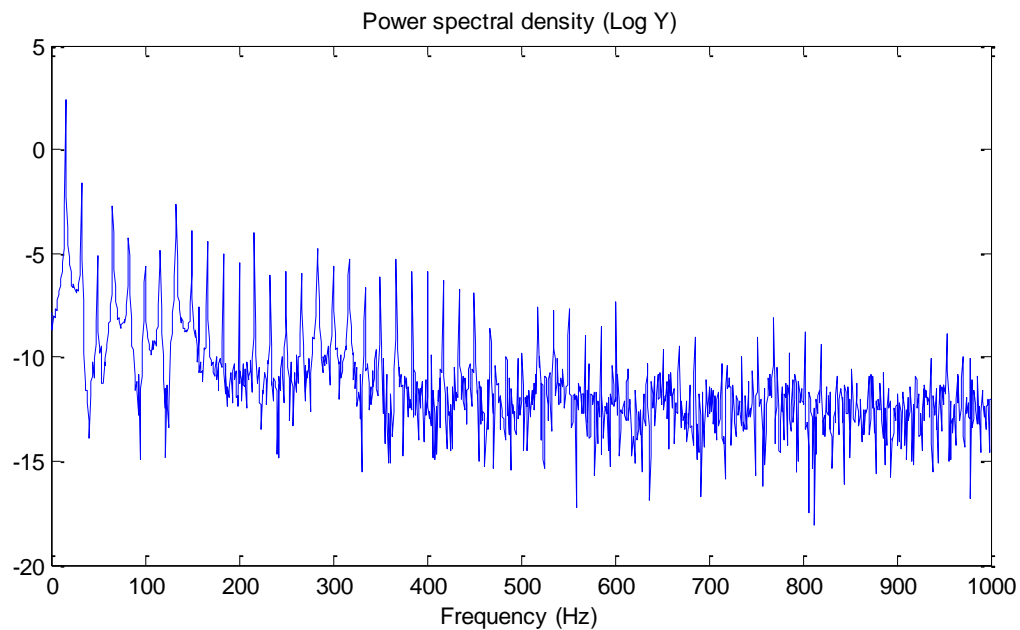


**Figure 4.14 – FFT plot of spindle vibration in the Z-Axis direction when rotating at 1000rpm**

Figure 4.15 displays a zoomed in section of the frequency plot to show the clear domination of the rotational frequency of 16.67 Hz.

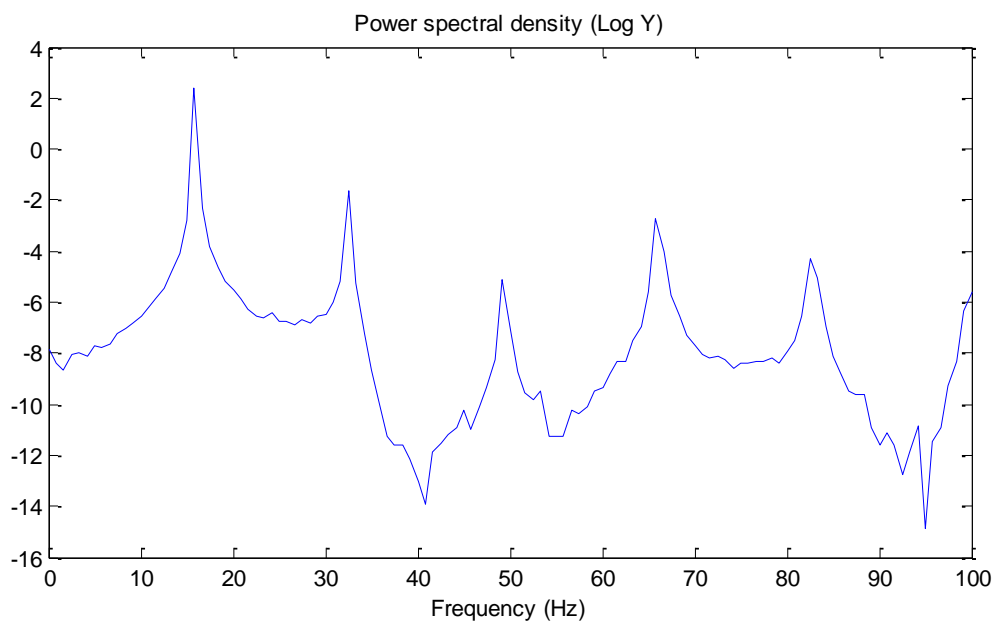


**Figure 4.15 – Zoomed in FFT plot of spindle vibration in the Z-Axis direction when rotating at 1000rpm**

### 4.3. Chapter Conclusions

The sensor selection is only part of the problem, the rest of the hardware and software is just as important. The use of suitable test-bars and fixtures is essential to enable high accuracy measurement to take place.

Once the hardware is capable of logging data, data processing is still required to convert the captured data to a format that can be understood and presented in accordance with ISO standards. This section described the processes required for processing data from thermal, geometric and vibration analysis testing.

A full list of the required hardware and software to enable spindle analysis to be performed can be found in table 6:

**Table 6 – Spindle Analysis B.O.M**

<b>Hardware</b>		
<b>Item</b>		<b>Quantity</b>
Non-Contact Displacement Sensors		6
Signal Amplifier		6
Data Acquisition Device		1
Power Supply		1
Sensor Fixture		1
20mm Test Bar (short)		1
20mm Test Bar (long)		1
Tool Holders	HSK 100	1
	HSK 63	1
	ISO 50	1
	SK 40	1
	SK 50	1
	Capto	1
Temperature Sensors		12
Temperature Sensor USB Adapter		1
Temperature Sensor Extension Cables		4
Adapter Power Cable		1
Thermal Imaging Camera		1
<b>Software</b>		
WinTcal (temperature logger)		1
NI Signal Express		1
Compiled Matlab functions		1

## 5.0 Practical Spindle Analysis

---

This section looks at real case studies of spindle analysis taken in typical manufacturing environments. It identifies potential drawbacks of the newly employed system and how they can be overcome.

### 5.1. In situ Calibration

From practical experience, it is not always possible to use the same target material when performing spindle measurements. In many cases different machines will have differing test bar material. In certain situations it may be necessary to perform a measurement against a component mounted in a spindle. With this in mind a simple in-situ method for calibrating the sensor to the necessary target material is extremely beneficial

The linear scale of a machine tool is specified with linear errors on a typical modern machine in the region of 5  $\mu\text{m}/\text{m}$ , so when calibrating over 0.1 mm, any error can be considered negligible. There is a possibility of stiction error when moving the machine in small increments but experience shows that this is typically negligible but may be the case on some older machines and as such, calibration, where possible, should take place on newer machine tools or where responsiveness has been ascertained.

To ensure the stability and accuracy of the measurement the following is taken into consideration:

- The accuracy and responsiveness of the axis over the region to be used must first be established by standard methods.
- Before any measurement is taken, it is important to move the axis of the machine over the region in which the measurement is to be taken to lubrication of the guide ways to counter the stiction.
- All calibration measurement is taken when approaching the target from the same direction so that no reversal error is introduced; an axis over-run [7] before the test ensures unidirectional calibration.



## 5.2. Thermal Analysis

Thermal analysis of machine tool spindles is a good way of setting up a thermal profile of the machine to allow for the errors, or for compensation to be applied during production.

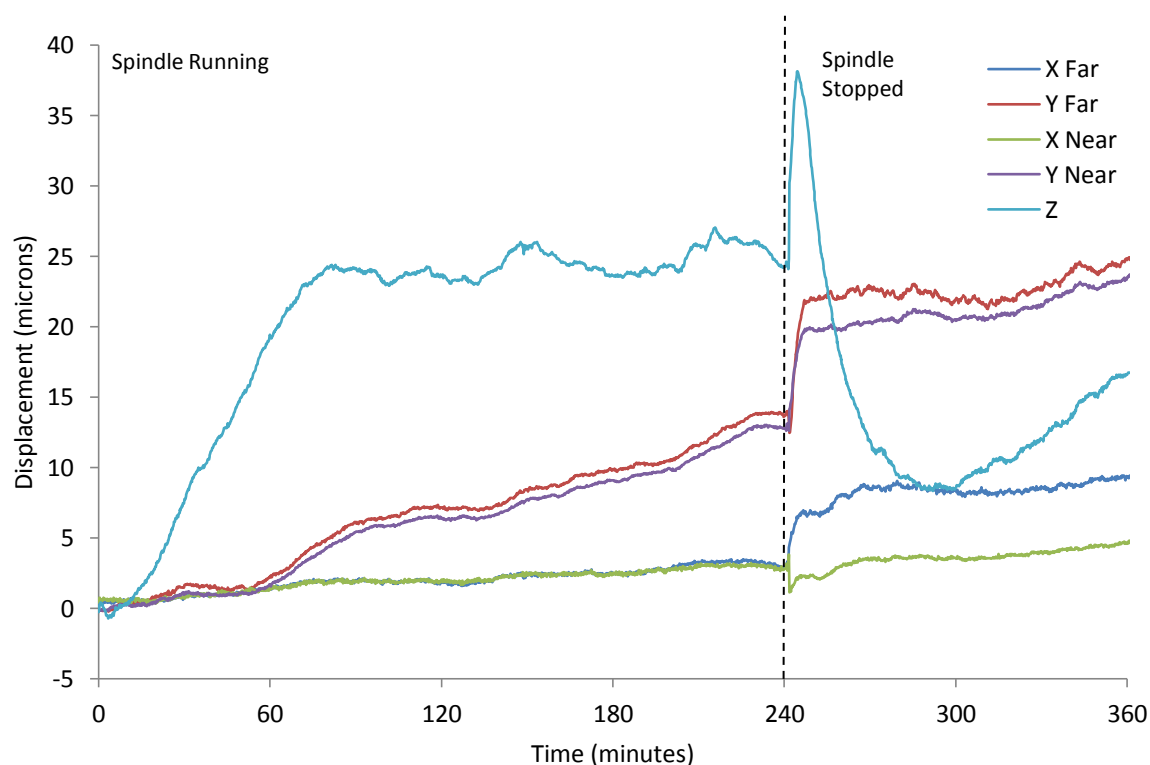


Figure 5.1 – Spindle displacement during a 6 hour spindle heating test

Figure 5.1 shows the displacement of a milling spindle in relation to the table when running at a constant 5000rpm for a 4 hour period. The largest displacement is in the Z direction where the spindle displaces by 25  $\mu\text{m}$  over the first 80 minutes, it then remains stable to within 4  $\mu\text{m}$  for the remaining run time.

In addition, once the spindle is stopped there is a rapid increase in displacement, up to 38  $\mu\text{m}$ , before retracting back. This is most likely due to residual heat from the test flowing into and expanding the test-bar, therefore increasing the displacement.

While monitoring the displacement of the spindle with the non-contact displacement sensors, it is also important to measure the temperature of the spindle at various locations. The ISO standard suggests monitoring the surface temperature at the spindle nose as well as the ambient temperature of the spindle and machine. This is considered to be the minimum data, the more temperature sensors used the better the thermal profile that can be obtained.

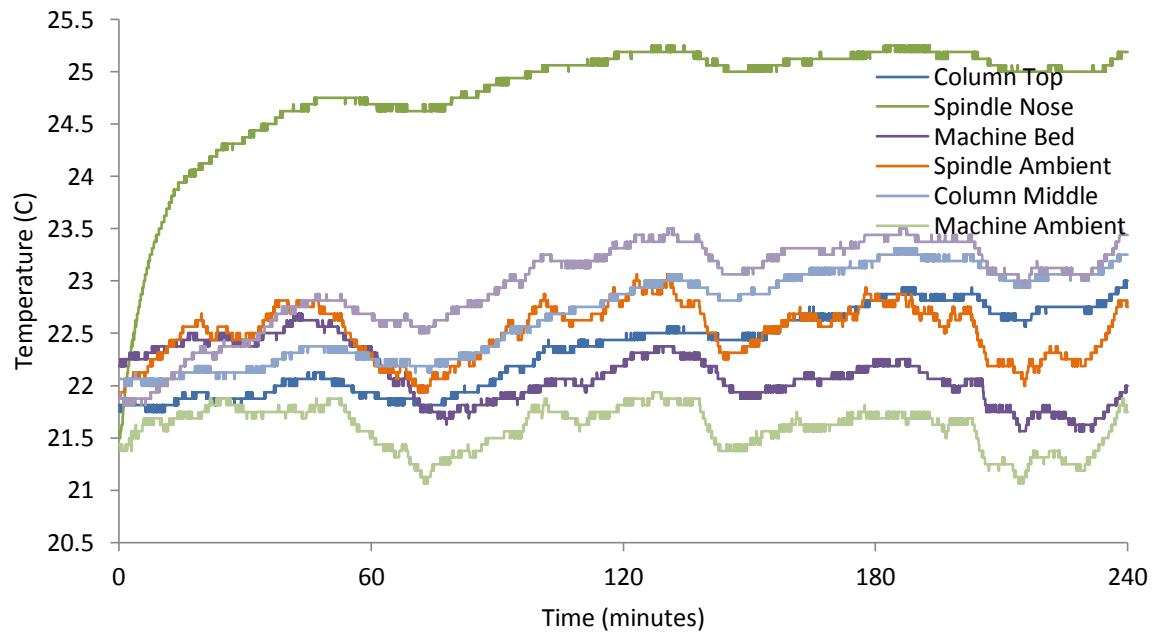


Figure 5.2 – Spindle temperature during a 6 hour spindle heating test

Figure 5.2 shows the temperature of the spindle and surrounding area during the 6 hour heating test. When compared to the displacement data, there is a direct correlation between the temperature at the spindle nose and displacement in the Z direction, as can be seen in figure 5.3. The temperature at the spindle nose quickly heats up to its maximum of around 25°C. It took slightly longer for the Z axis to achieve its maximum displacement but this could be due to the flow of heat into the test bar.

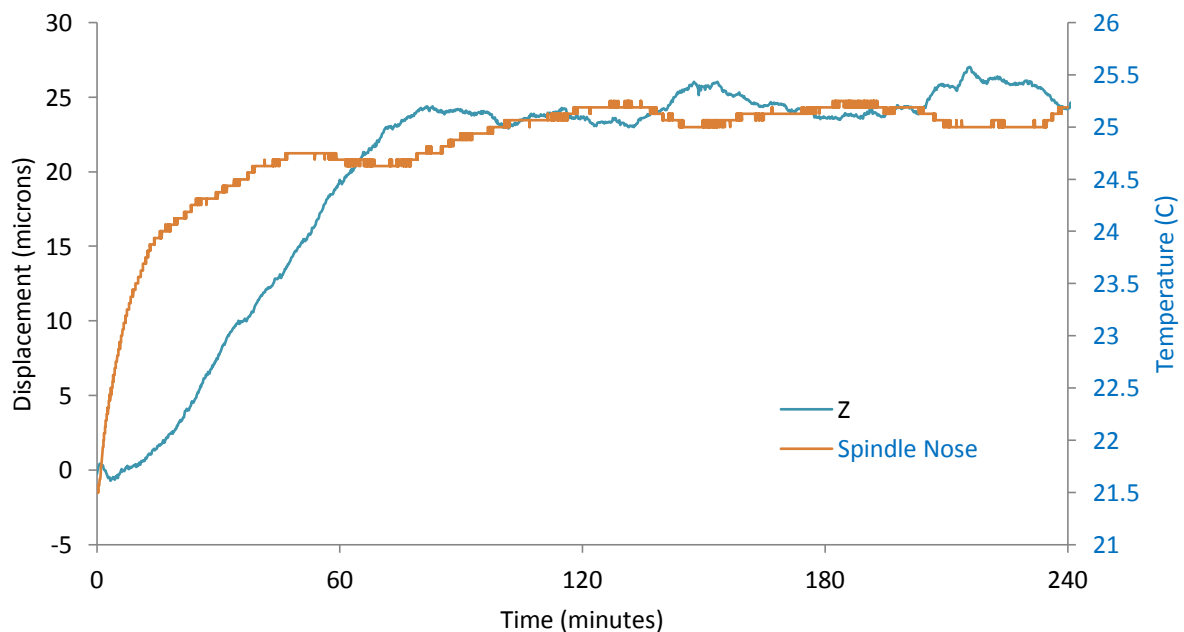


Figure 5.3 – Comparison of temperature and displacement during a 6 hour spindle heating test

### 5.2.1. Thermal Imaging

The use of thermal imaging during testing can also provide comprehensive data about the flow of heat through the structure of the machine tool by way of the high spatial resolution of temperature information. One drawback of thermal imaging is that the accuracy is dependent on the knowledge of the emissivity of the surfaces being measured. Also, a typical specification for a camera is in the order of  $\pm 2^{\circ}\text{C}$ . Methods exist to improve this accuracy, including applying masking tape (with a known emissivity of 0.95) to areas of thermal interest and averaging the images to reduce noise. Accurate surface mountable temperature sensors in the field of view of the camera can also be used to adjust emissivity to improve accuracy. Figure 5.4 shows thermal images taken at different periods during a spindle heating test on a large vertical turning machine.

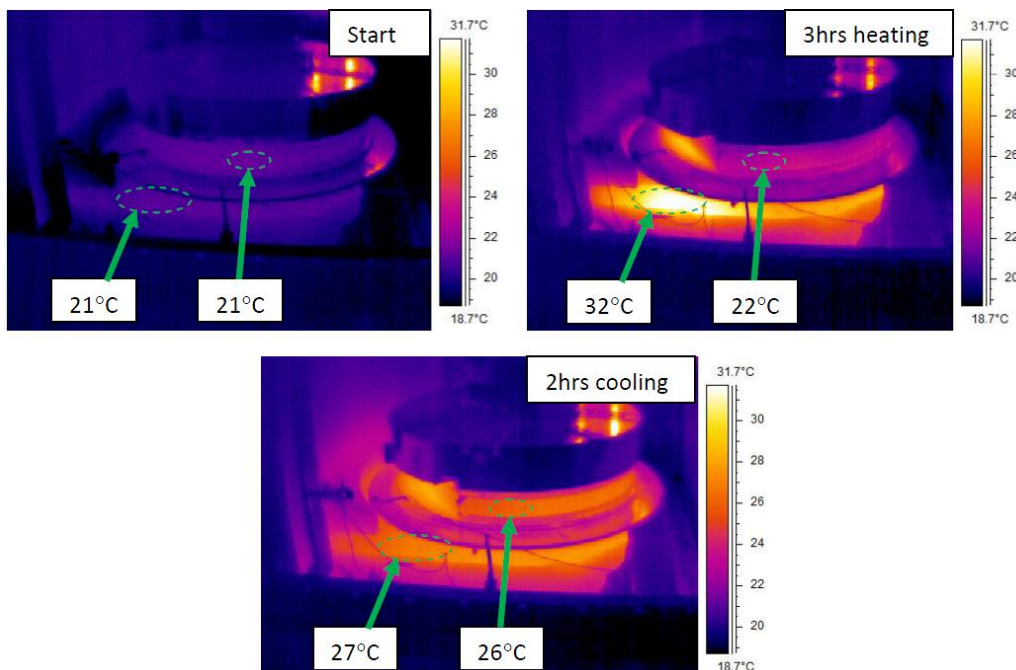


Figure 5.4 – Thermal imaging at various times of a heating and cooling test

Using the test methods described in ISO230 part 3 “determination of thermal effects”, combined with thermal imaging sequences, data can be obtained to establish a thermal profile of a machine tool in its operational environment. This data can then be used to establish production capability, corrective action or when creating thermal compensation files to compensate out any thermal error present in the machine.

### 5.3. Geometric Analysis

Geometric analysis of a machine tool spindle involves measuring the error motion of the spindle (see section 4.2.2).

The example in this section is measuring the radial error motion of a high precision air bearing spindle. Using the Donaldson reversal technique described in the previous section, two sets of data were captured.

Figure 5.5 shows 20 revolutions of a test-bar from setup 1(see section 4.2.2.1) of the reversal measurement plotted together.

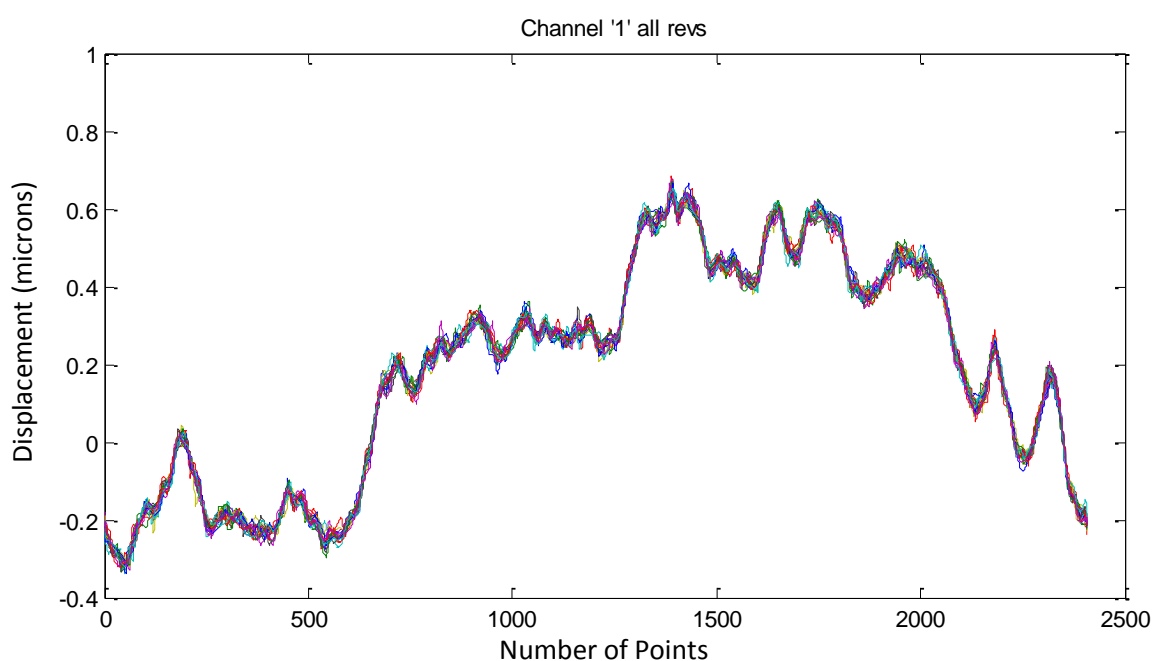


Figure 5.5 – All run plotted from run 1

The data includes test-bar run-out, form error, electrical run-out error and spindle error. The largest error can be seen as the test-bar run-out, which is approximately  $1\mu\text{m}$ . The rest of the errors require separation using the reversal technique.

Figure 5.6 shows 20 revolutions of a test-bar from setup 2 of the reversal measurement plotted together. The data includes test-bar run-out, form error, electrical run-out error and spindle error.

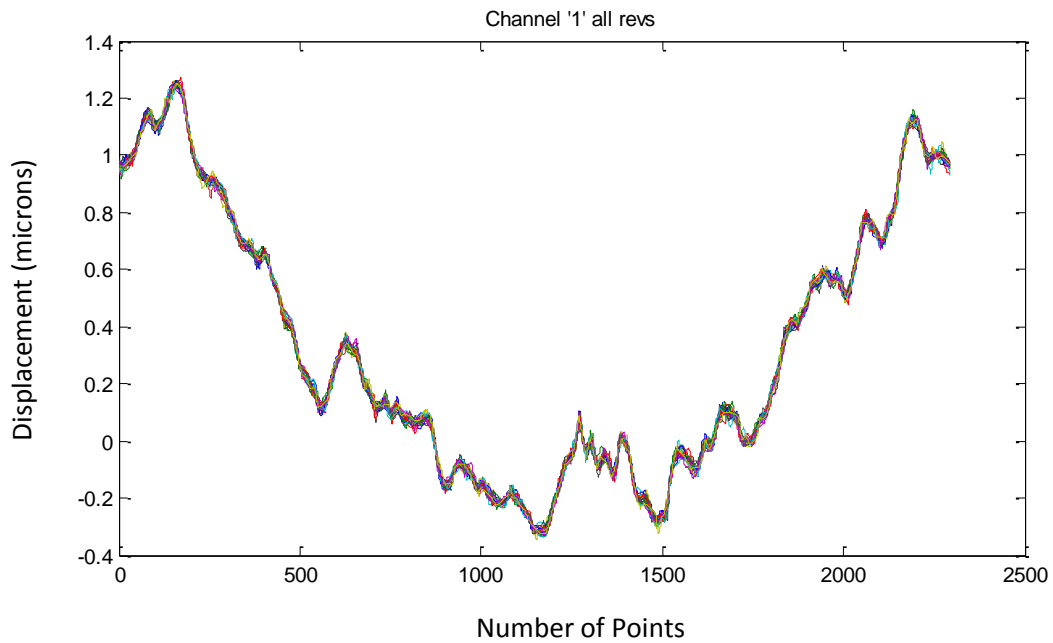


Figure 5.6 – All runs plotted from run 2

These two sets of data are then input in the Donaldson reversal formulas (see page 60) to separate the errors so that the remaining spindle error can be plotted on a polar plot and the asynchronous and synchronous error motion values can be calculated.

Asynchronous error motion is the non-repeating change in position of the spindle on successive rotations.

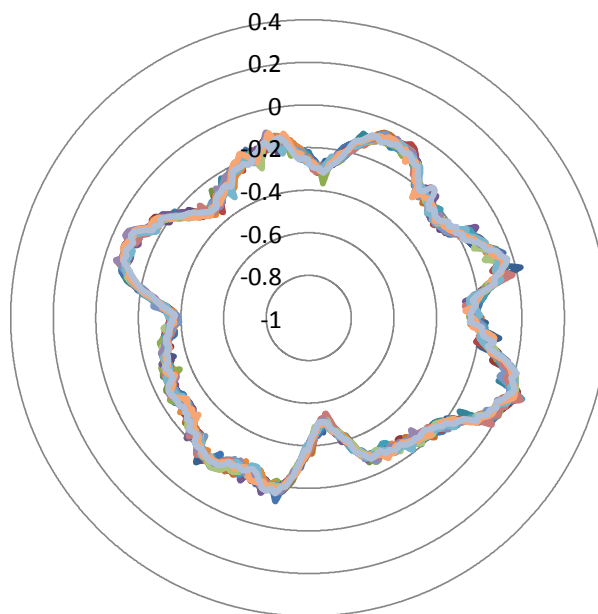
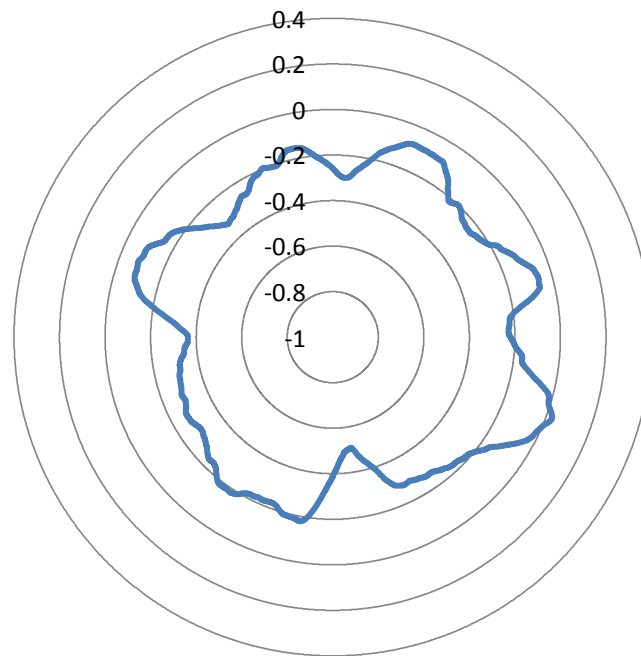


Figure 5.7 – All runs plotted in a polar plot

The asynchronous error value is the difference between the maximum and minimum values at a particular angle in the above plot. A description of this can be seen in figure 2.3 on page 17. In this case it is 0.13  $\mu\text{m}$ .

Synchronous error is the once per revolution error that occurs as a result of the spindles deviation from its true centre line. It characterises the spindle ability to cut a round hole. Figure 5.8 shows the synchronous error plot, which is an average of the 20 revolutions.



**Figure 5.8 – Averaged data run-out plot**

The synchronous error value is the difference between the maximum and minimum values in the above plot. In this case it is 0.53  $\mu\text{m}$ .

## 5.4. Vibration Analysis

Vibration analysis can be linked to the asynchronous error motion values to identify the frequency at which vibration may be occurring.

The vibration data in figure 5.9 is from an air bearing spindle being run at 250rpm. The first big peak at 4.16Hz is due the rotational frequency of the spindle.

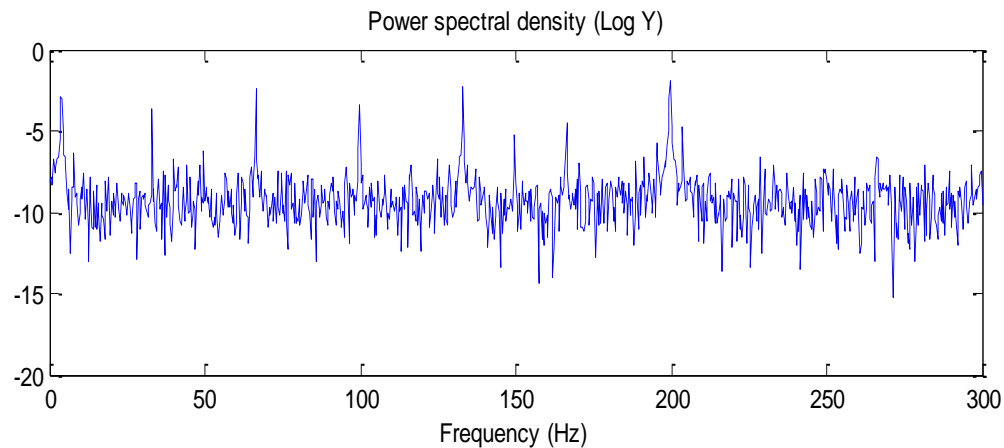


Figure 5.9 – Vibration data from an air bearing spindle running at 250rpm

The 5.10 shows the same air bearing spindle being run at 500rpm. As can be seen, the first big peak is at 8.3 Hz; again this is due to the rotational speed of the spindle. Some of the vibration peaks occur at the same frequency as the previous plot, such as at 67 Hz and 200Hz. This suggests that this is vibration due to the resonant frequencies of the spindle and surrounding structure.

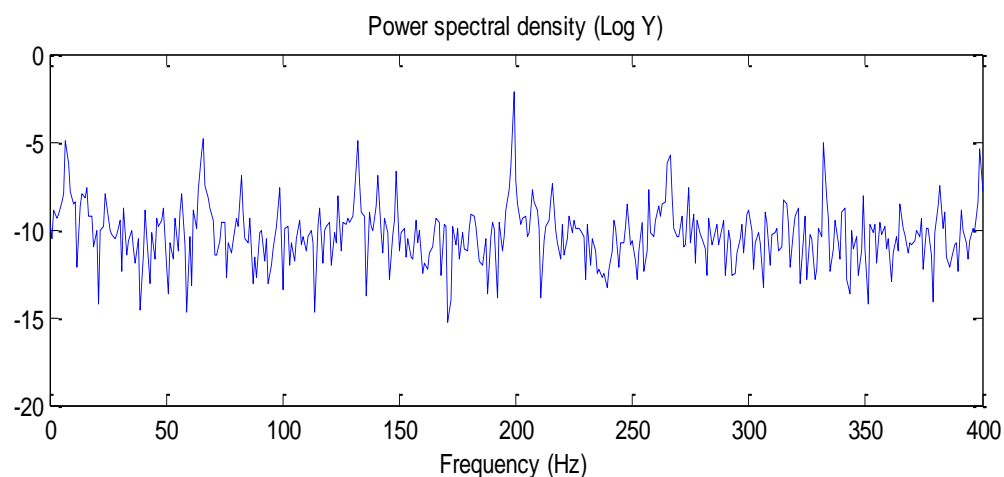


Figure 5.10 – Vibration data from an air bearing spindle running at 500rpm

Further examples of practical spindle analysis can be found in the appendix.

## 6.0 Conclusions

---

Research was conducted into relevant work in the area of spindle metrology. With it being a relatively new concept there was a limited amount of directly related work available to assess. However, there was a substantial amount of work in related fields such as structural vibration, this coupled with the appropriate ISO standards aided with the research process.

The non-contact sensing technologies, suggested in the ISO standards as suitable for use in spindle analysis, were investigated to find the most appropriate solution for an affordable system useable on a regular basis by maintenance engineers in a typical workshop environment. This investigation involved extensive research and testing to assess the sensors against their manufacture specifications.

This resulted in eddy current and capacitance sensors being confirmed as appropriate for spindle analysis testing, but with the laser triangulation sensors not meeting the required dynamic resolution. In the end eddy current sensors were chosen as the most appropriate solution, for the following reasons:

- They can be used in manufacturing environments where swarf, dust and coolant may be present.
- They offered a much cheaper solution, which was important as the sensors make up a large percentage of the overall system cost.

The overall outcome was the design and development of an affordable spindle analysis system that can be taken into a manufacturing environment to perform comprehensive spindle analysis testing and post processing of data. A critical contribution from this solution is the ability to measure very small errors from, for example an air bearing or high quality rolling element bearing spindle to large thermal errors using a single system.



## 7.0 Future Work

---

As described and demonstrated in this work, the designed system is capable of performing robust spindle analysis. However, further development of both system hardware and software would be beneficial to improve the efficiency of measurement and data processing.

### 7.1. Test-bar Design and Holding

Manufacturing a set of invar test-bars would improve the thermal properties and enable more accurate thermal error measurement, without the influence of thermally expanding test-bars. However, while this is an improvement for the thermal error measurement, further testing will be required to assess the permeability of invar and whether or not this would have an effect on accuracy during the geometric testing.

A set of tool holders would be a good addition to the system, to hold the test-bars when measuring milling spindles. Figure 7.1 shows a commercially available tool holder that can be adjusted to remove the run-out of the test-bar.



Figure 7.1 – Adjustable tool holder to 0.000 $\mu$ m run-out [39]

Being able to centre the test bar would reduce vibration when running at high speeds and allow for more accurate measurement of high precision spindles.

When measuring turning spindles with face plate mounting, an interface holder can be developed with the same idea of being able to adjust the test-bar to remove the run-out. This would also result in a much quicker test setup than the current method, therefore improving testing efficiency and minimising machine downtime.

## 7.2. Fixtures

The manufacture of one Invar fixture that could be used for all the testing would reduce setup time between tests as the same fixture would be used and also provide thermal stability during thermal testing.



Figure 7.2 – Ultrafine adjustment screws [40]

The fixture would need to be fully adjustable, allowing for very fine movements during precision test setups. Figure 7.2 shows a set of ultrafine adjustment thumb screws, which allow for an adjustment sensitivity of  $0.5\mu\text{m}$ .

### **7.3. Data Processing Software**

The current data processing method is run as a series of script files. This is easy to use but can sometimes be quite time consuming. An ideal solution would be to compile an executable application that can run all the scripts from one place easily.

The inclusion of a sensitivity displays would also be beneficial, so that the most sensitive part of the individual sensors range can easily be identified and positioned.

### **7.4. Test Methodology**

Further investigation in to the multi probe method would be beneficial to establish if the additional cost of purchasing additional sensors required can be offset by the time saved from reduced setup times of tests.

## 8.0 References

---

- [1] Abele, E. Altintas, Y. Brecher, C. "Machine Tool Spindle Units", CIRP Annals – Manufacturing Technology, 2010.
- [2] ISO 230-3, Test code for machine tools – Part 3: Determination of thermal effects. 2007.
- [3] ISO 230-7, Test code for machine tools – Part 7: Geometric accuracy of axes of rotation. 2006.
- [4] ISO 230-8, Test code for machine tools – Part 8: Determination of vibration levels. 2009.
- [5] Lion Precision, "Capacitive sensor operation and optimisation", TechNote LT03-0020, 2011.
- [6] Nabavi, MR "A novel interface for eddy current displacement sensors", IEEE transactions on instrumentation and measurement, vol. 58, no.5, May 2009.
- [7] Lion Precision, "Difference between capacitive and eddy current sensors", TechNote LT05-0011, 2009.
- [8] Lion Precision, "Calibration of eddy current sensors", Eddy current TechNote LT02-0013, 2007.
- [9] Yating, Y. "Investigation on contribution of conductivity and permeability on electrical runout problem of eddy current displacement sensor", 2011.
- [10] Teruhiro, K. "High frequency permeability of ferromagnetic metal composite materials", Journal of magnetism and magnetic materials 310, pp 2566 – 2568, 2007.
- [11] Ma, X. "Eddy current measurements of electrical conductivity and magnetic permeability of porous metals", NDT & E International 39, pp 562 – 568, 2006.
- [12] Bryan, J. International status of thermal error research. Annals of the CIRP, Vol. 39, Part 2, 645-656, 1990.
- [13] Postlethwaite, S. "Machine tool thermal error reduction – an appraisal, Journal of Engineering Manufacture, 1999.
- [14] Ramesh, R. Error compensation in machine tools – a review: Part II: thermal errors. International Journal of Machine Tools and Manufacture, Vol 40, Issue 9, 1257-1284, 2000.
- [15] Mian NS, Fletcher SF, Longstaff AP, Myers A, 2011 'Efficient thermal error prediction in a machine tool using finite element analysis', *Measurement Science and Technology*, 22(8): p. 085-107.
- [16] Fletcher S, Longstaff AP and Myers A, 2007 'Measurement methods for efficient thermal assessment and error-compensation' *Proceedings of the Topical Meeting: Thermal Effects in Precision Systems – Maastricht*.
- [17] Longstaff AP, Fletcher S, and Ford DG, 2003 'Practical experience of thermal testing with reference to ISO 230 Part 3', *Laser Metrology and Machine Performance VI*: p. 473-483.

- [18] Jywe, WY. "The development of high speed spindle measurement system using laser diode and a quadrants sensor", *International journal of machine tools and manufacture* 45, 2005: p1162-1170.
- [19] Castro, HFF. "A method for evaluating spindle rotation errors of machine tools using a laser interferometer", *Measurement* 41, 2008: p526 - 537.
- [20] Marsh, E. *Precision spindle metrology*, second edition, DEStech Publications Inc, 2010.
- [21] Lu, X. "A new method for characterising axis of rotation radial error motion: Part 1 two-dimension radial error motion theory", *Precision Engineering*, 2011.
- [22] Lu, X. "A new method for characterising axis of rotation radial error motion: Part 2 Experimental results", *Precision Engineering*, 2011.
- [23] Marsh, E. "A comparison of reversal and multiprobe error separation", *Precision Engineering* 34, pp 85 – 91, 2010.
- [24] Martin, D.L. "Precision spindle bearing error analysis", *International journal of machine tools & manufacture* vol 35, pp187 – 193, 1995.
- [25] Vafaei, S. "Vibration monitoring of high speed spindles using spectral analysis techniques",
- [26] Felten, D. "Understanding bearing vibration frequencies" 2003.
- [27] ISO Standard 76-1987, Load ratings and fatigue life, 1987.
- [28] "ISO 281:2007 bearing life standard – and the answer is?", *tribology and lubrication technology*, 2010.
- [29] Bell, S. "A beginner's guide to uncertainty of measurement", *Measurement good practice guide* No. 11 Issue 2, 2001.
- [30] Flack, D. Hannaford, J. "Fundamental good practice in dimensional metrology", *Measurement good practice guide* No.80, 2005.
- [31] Wilson, JS. "Sensor technology handbook", Elsevier, 2005.
- [32] Shieh, J. "The selection of sensors", *Progress in materials science* 46, pp 461 – 504, 2001.
- [33] Lai, Y. "Eddy current displacement sensor with LTCC technology," Ph.D. dissertation, Universität Freiburg, Switzerland, 2005.
- [34] Tian. G. Y, Zhao. Z. X and Baines. R.W, "The research of inhomogeneity in eddy current sensors", *Sens. Actuators A, Phys.*, vol. 69, no. 2, p148– 151, Aug. 1998.
- [35] Zhang, H. "An approach of eddy current sensor calibration in state estimation for maglev system", *Electrical machines and systems*, p1955-1958, 2007.
- [36] Rao, BPC. "Practical eddy current testing", Oxford: Alpha Science, 2007.
- [37] Kang, Y. "Integrated CAE strategies for the design of machine tool spindle bearing systems", *Finite Element in Analysis and Design* 37, 2001.
- [38] *International journal of machine tools & manufacture* vol 42, pp1223 – 1234, 2002.

- [39] <http://www.mtiinstruments.com/products/lasertriangulation.aspx>
- [40] [http://www.gb.schunk.com/schunk/schunk\\_websites/news/press\\_release\\_detail.html?article\\_id=15440&submenu=3700&submenu2=244&archive=2010&country=GBR&lngCode=EN&lngCode2=EN](http://www.gb.schunk.com/schunk/schunk_websites/news/press_release_detail.html?article_id=15440&submenu=3700&submenu2=244&archive=2010&country=GBR&lngCode=EN&lngCode2=EN)
- [41] [http://www.standa.lt/products/catalog/fine\\_adjustment?item=179](http://www.standa.lt/products/catalog/fine_adjustment?item=179)

## 9.0 Appendix

---

	Page
Micro Epsilon Eddy Current Testing	86
Further Examples of Practical Spindle Analysis	88

## 9.1. Micro Epsilon Eddy Current Testing

### Linearity Test

Figure 9.1 shows the output of the micro epsilon eddy current sensor, with the sensor output is plotted in blue and a linear fit is plotted in red. The linear fit is very close to that of the sensor output, showing that the sensor has a very good linear output over its full range.

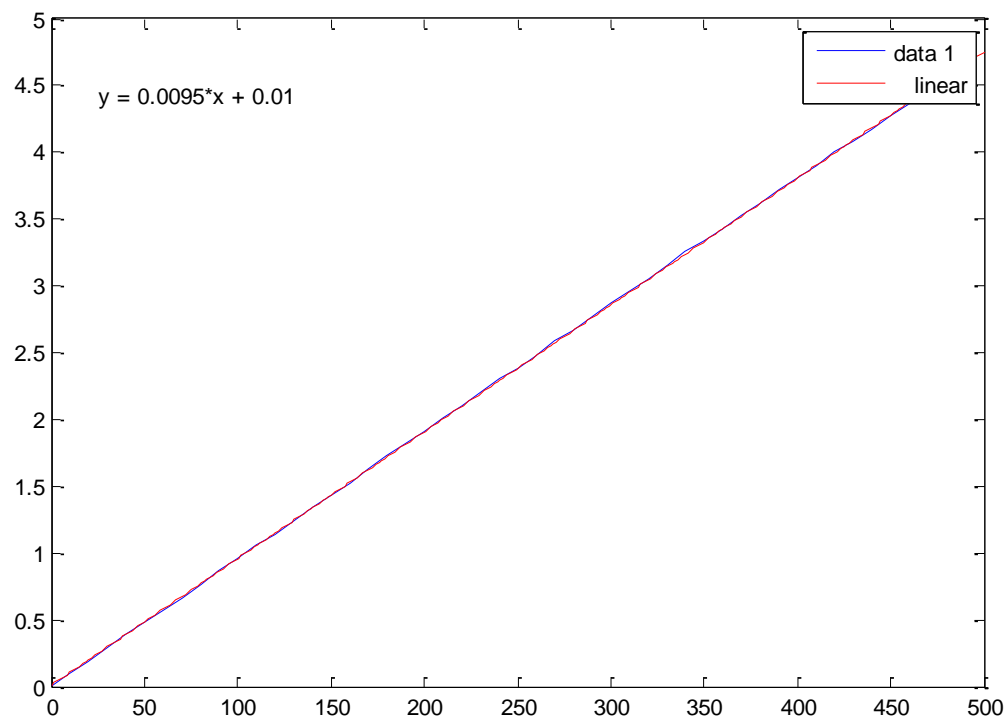
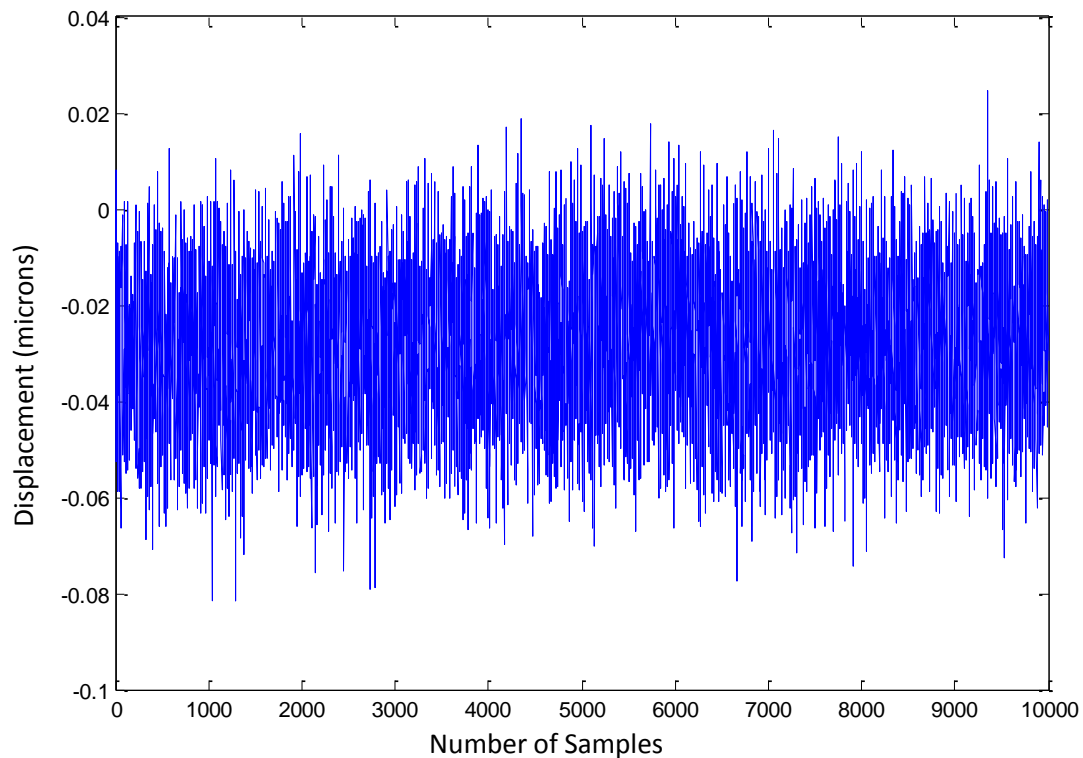


Figure 9.1 – Linearity of Micro-Epsilon eddy current sensor



## Static Resolution Test

The static resolution test was carried out using the same methodology as with the Kaman eddy current sensors.



**Figure 9.2 – Stability of Micro-Epsilon eddy current sensor**

Figure 9.2 shows the static displacement to be approximately 50nm which is what was suggested by the manufacturer specification. This would be a good enough resolution to measure the majority of machine tool spindles. When standard deviation is applied to this data it identifies a potential resolution of 14.3nm.

This test was repeated at various positions in the sensor range with the following results:

**Table 7 – Potential Resolutions at various positions in the sensor range**

Distance from start of range ( $\mu\text{m}$ )	Potential resolution when standard deviation is applied to the data (nm)
170	12.5
300	15.9
500	24
800	47.2

## 9.2. Further Examples of Practical Spindle Analysis

### Thermal Step Heating Test

Figure 9.5 shows the displacement data from a thermal step heating test carried out on a ball bearing spindle. The spindle was run at 500, 1000, 2000 and 3000 rpm for 1 hour periods and then left to cool.

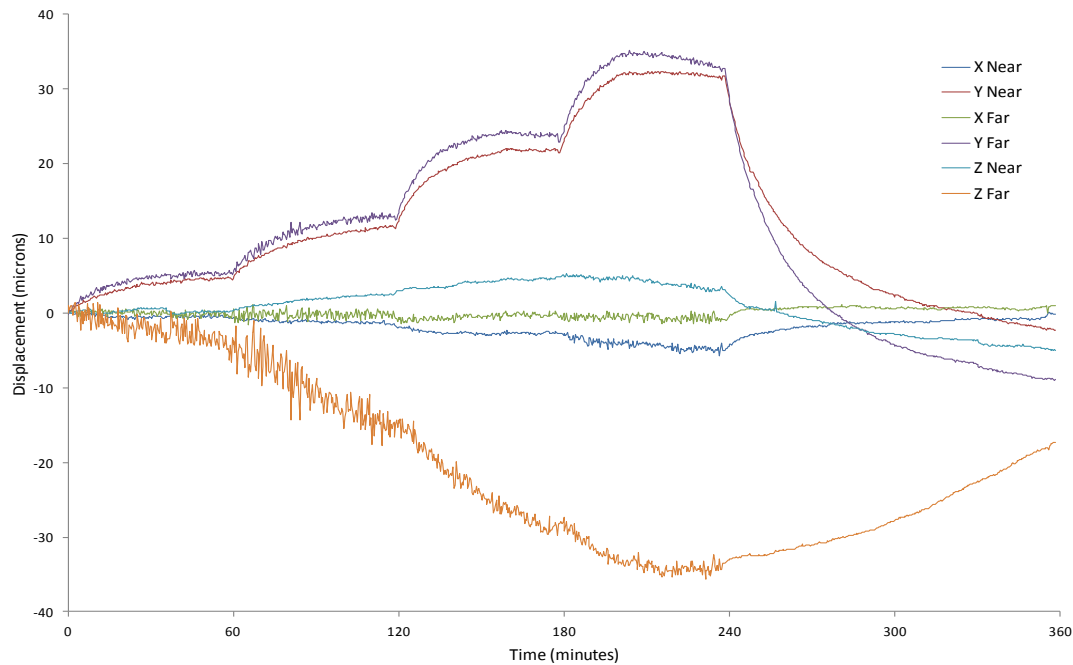


Figure 9.3 – Thermal step heating test displacement measurement

Displacement is positive for increasing distance between the sensor head and the spindle nose.

The maximum spindle displacement during the 6-hour test was 34  $\mu\text{m}$  in the Z-axis direction, 5  $\mu\text{m}$  in the X-axis direction and 34  $\mu\text{m}$  in the Y-axis direction.

The above plot also shows the displacement of the spindle stabilises during each of the 1 hour run times at the different speeds.

This sort of data provides good information to users about potential warm up cycles and thermal compensation to be applied.

Figure 9.6 shows the temperature data from the same thermal step heating test carried out on a ball bearing spindle.

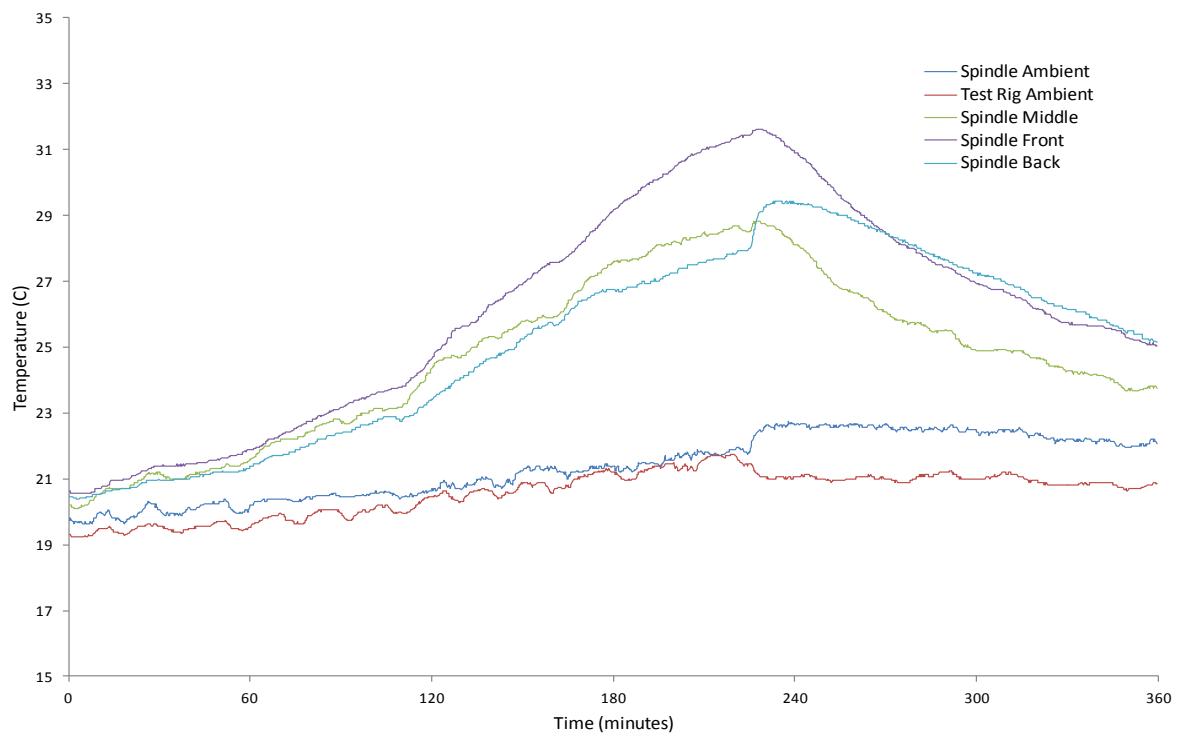


Figure 9.4 – Thermal step heating test temperature measurement

Figure 9.7 shows the thermal images for the same test which can be used for verification of the temperature data.

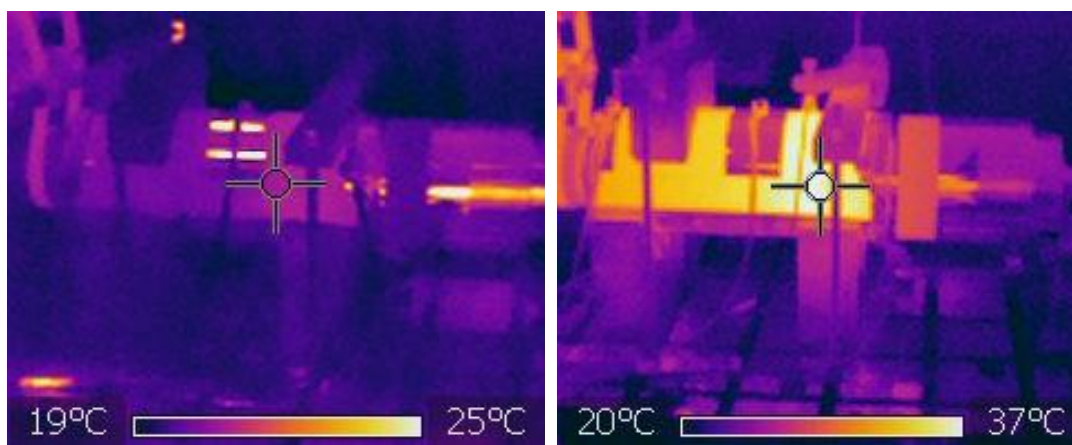


Figure 9.5 – Thermal step heating test thermal imaging

Figure 9.8 shows a correlation between the spindle displacement and the spindle ambient temperature.

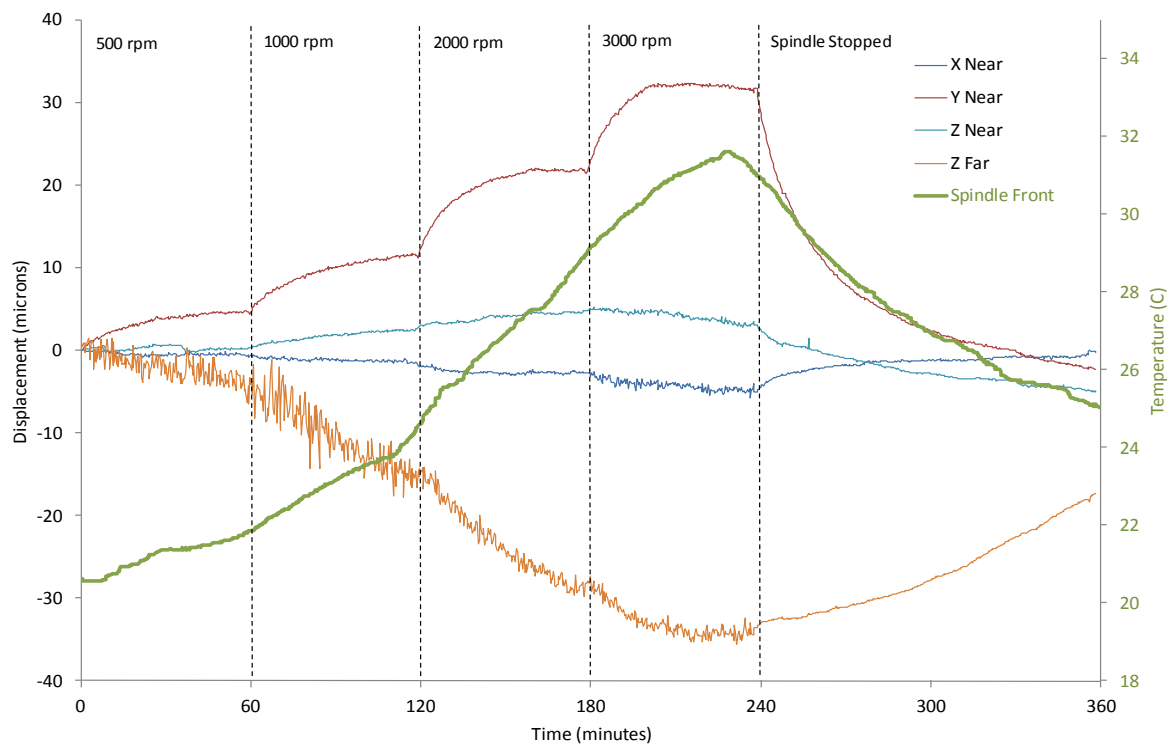
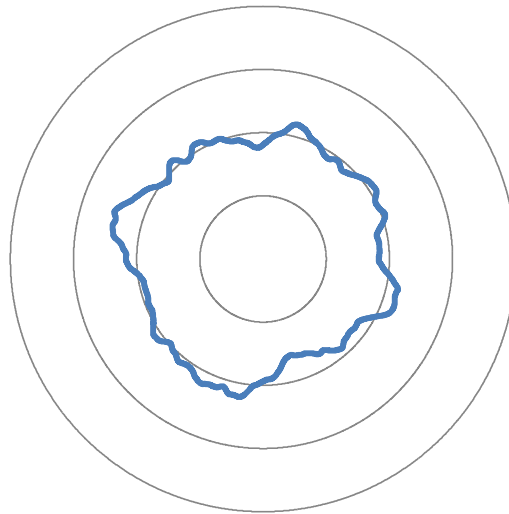


Figure 9.6 – Thermal step heating test temperature and displacement comparison

## Error Motion Tests

A radial error motion test of carried out on a mechanical ball bearing spindle while running at 1000rpm.



0.5μm / division

**Figure 9.7 – Radial run-out of ball bearing spindle at 1000rpm**

Figure 9.9 shows a polar plot of the averaged data from 20 runs, as per the ISO standard, to show the synchronous error. In this case it was 0.64μm, which is very good for a mechanical spindle and shows the requirement for very resolution sensors to be used.

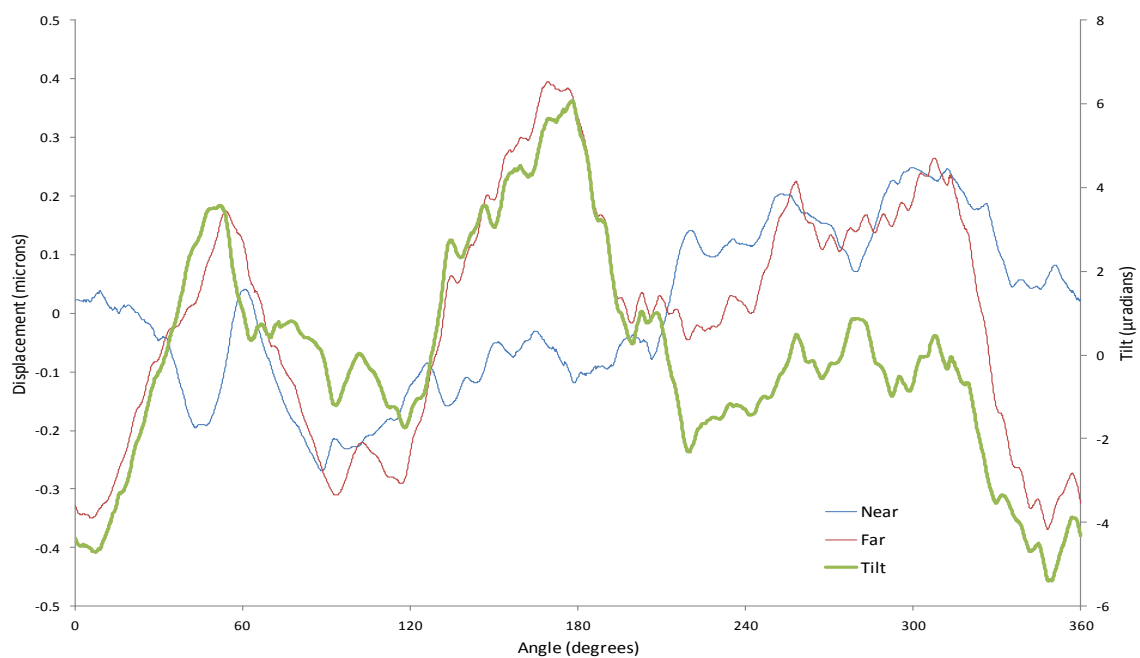


**Figure 9.8 – Tilt error of ball bearing spindle at 1000rpm**

Figure 9.10 shows the tilt error measurement from the same spindle when running at 1000rpm. This identifies a further element of required further work; to develop polar plots to display the tilt error is a clearer way.

### Vibration Analysis

Vibration data was also logged from the same ball bearing spindle when it was running at 1000rpm.

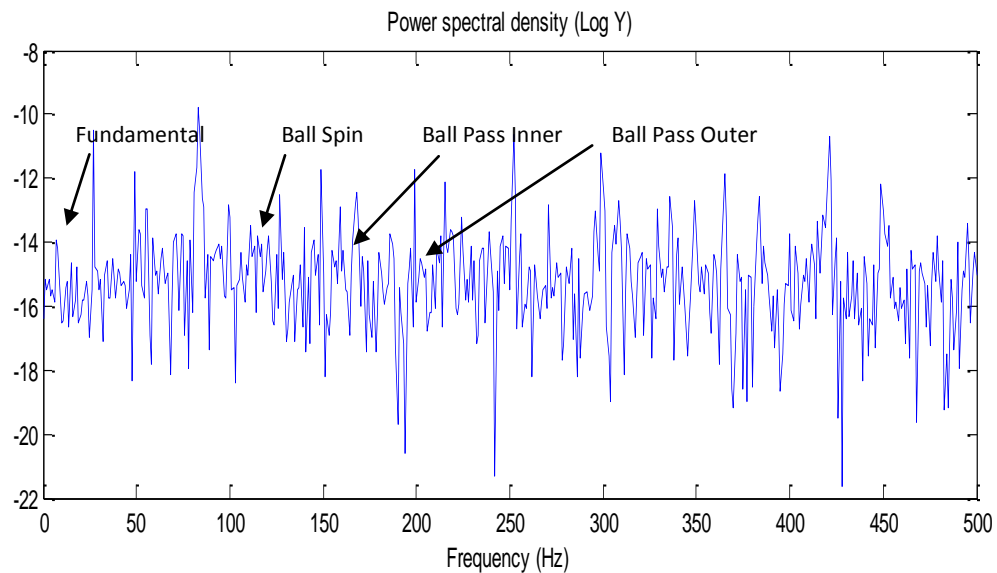


**Figure 9.9 – Vibration of ball bearing spindle at 1000rpm**

Figure 9.11 shows the FFT plot for the vibration data with the frequencies of interested identified, that are related to the ball bearing sets used in the spindle.